

OPEN ACCESS

EDITED BY

Biao Jin,
Yangzhou University, China

REVIEWED BY

Georg Leitinger,
University of Innsbruck, Austria
Raquel Lobo-do-Vale,
University of Lisbon, Portugal

*CORRESPONDENCE

Yafei Li

✉ l.yafei@outlook.com;

✉ yafei.li@usys.ethz.ch

RECEIVED 02 January 2023

ACCEPTED 04 April 2023

PUBLISHED 09 May 2023

CITATION

Li Y, Eugster W, Riedl A, Lehmann MM,
Aemisegger F and Buchmann N (2023)

Dew benefits on alpine grasslands
are cancelled out by combined
heatwave and drought stress.

Front. Plant Sci. 14:1136037.

doi: 10.3389/fpls.2023.1136037

COPYRIGHT

© 2023 Li, Eugster, Riedl, Lehmann,
Aemisegger and Buchmann. This is an open-
access article distributed under the terms of
the [Creative Commons Attribution License
\(CC BY\)](https://creativecommons.org/licenses/by/4.0/). The use, distribution or
reproduction in other forums is permitted,
provided the original author(s) and the
copyright owner(s) are credited and that
the original publication in this journal is
cited, in accordance with accepted
academic practice. No use, distribution or
reproduction is permitted which does not
comply with these terms.

Dew benefits on alpine grasslands are cancelled out by combined heatwave and drought stress

Yafei Li^{1*}, Werner Eugster¹, Andreas Riedl¹,
Marco M. Lehmann², Franziska Aemisegger³
and Nina Buchmann¹

¹Institute of Agricultural Sciences, ETH Zurich, Zurich, Switzerland, ²Forest Dynamics, Swiss Federal Institute for Forest, Snow and Landscape Research (WSL), Birmensdorf, Switzerland, ³Institute for Atmospheric and Climate Science, ETH Zurich, Zurich, Switzerland

Increasing frequencies of heatwaves combined with simultaneous drought stress in Europe threaten the ecosystem water and carbon budgets of alpine grasslands. Dew as an additional water source can promote ecosystem carbon assimilation. It is known that grassland ecosystems keep high evapotranspiration as long as soil water is available. However, it is rarely being investigated whether dew can mitigate the impact of such extreme climatic events on grassland ecosystem carbon and water exchange. Here we use stable isotopes in meteoric waters and leaf sugars, eddy covariance fluxes for H₂O vapor and CO₂, in combination with meteorological and plant physiological measurements, to investigate the combined effect of dew and heat-drought stress on plant water status and net ecosystem production (NEP) in an alpine grassland (2000 m elevation) during the June 2019 European heatwave. Before the heatwave, enhanced NEP in the early morning hours can be attributed to leaf wetting by dew. However, dew benefits on NEP were cancelled out by the heatwave, due to the minor contribution of dew in leaf water. Heat-induced reduction in NEP was intensified by the combined effect of drought stress. The recovery of NEP after the peak of the heatwave could be linked to the refilling of plant tissues during nighttime. Among-genera differences of plant water status affected by dew and heat-drought stress can be attributed to differences in their foliar dew water uptake, and their reliance on soil moisture or the impact of the atmospheric evaporative demand. Our results indicate that dew influence on alpine grassland ecosystems varies according to the environmental stress and plant physiology.

KEYWORDS

heatwave, dew, alpine grassland, drought, stable isotope, net ecosystem production

1 Introduction

A record-breaking heatwave struck Europe in June 2019 (Mitchell et al., 2019; WMO, 2019), one in a series of severe heatwaves and droughts since summer 2003 (Ciais et al., 2005), 2010 (Barriopedro et al., 2011), 2016 (Zschenderlein et al., 2018), and 2018 (Gharun et al., 2020). Drought often is associated with a concurrent heatwave that affects terrestrial ecosystems (Overpeck, 2013), creating a so-called compound extreme event or period (Zscheischler and Fischer, 2020; Zscheischler et al., 2020). Compared to forests, grasslands are less vulnerable to drought stress, because of their relatively stable water use efficiency (i.e., the ratio of gross primary productivity per unit ecosystem evapotranspiration; Wolf et al., 2013) during a drought period. However intense and prolonged droughts and heatwaves do negatively affect grasslands (e.g., Gharun et al., 2020). A heatwave increases evapotranspiration of grasslands, thereby relieving the vegetation from heat stress, but at the expense of available water supply, which becomes scarcer the longer the heatwave persists (Teuling et al., 2010). Cremonese et al. (2017) reported that the combined drought and heat stress caused a reduction of canopy greenness in a mountain grassland. Also, De Boeck et al. (2016) reported that a heatwave combined with drought stress caused a reduction in above-ground biomass of alpine grassland plants. Li et al. (2020) found that gross primary production (GPP) in a semi-arid grassland was reduced more by drought than by a heatwave. However, Gharun et al. (2020) showed very different responses to the 2018 summer drought (as compared to the previous two years) among temperate grasslands at different elevations, with annual GPP decreasing at lower elevations but increasing at the alpine elevation due to abundant soil water after snowmelt. Thus, our understanding of the response of grasslands to a compound extreme drought and heatwave is controversial, particularly for alpine grasslands.

Dew was widely observed across arid (Uclés et al., 2013), temperate (Jacobs et al., 2006) and tropical (Clus et al., 2008) ecosystems, and can contribute up to 0.7–0.8 mm of water per day (Beysens, 2018). Dew amounts were quantified by lysimeters (Riedl et al., 2022), eddy-covariance (Jacobs et al., 2006), and isotopic (Kim and Lee, 2011) approaches. Nocturnal dew formation and its evaporation in the early morning hours is expected to alleviate drought and heat stress imposed by a compound extreme event due to the following reasons: (1) Dew formation is driven by radiative cooling of plant canopies with stronger long-wave outgoing radiation than that of atmospheric air on clear and calm nights (Oke, 1970), hence relieving canopy heat stress. (2) High humidity conditions under dew formation and dew water films covering foliage reduce plant transpiration (Gerlein-Safdi et al., 2018). (3) Foliar uptake of dew droplets or atmospheric water vapor alleviates plant water stress (Boucher et al., 1995; Dawson and Goldsmith, 2018). (4) Leaf gas exchange during the morning hours — when dew evaporates — might be highly relevant to alleviate plant stress, since transpiration and photosynthesis during most of the day are strongly impaired during a compound heat-drought event (Gharun et al., 2020). Oliveira et al. (2021)

pointed out that evaporation of dew induced CO₂ loss of a maritime pine forest during the rain-free period after wildfire. On the contrary, Simonin et al. (2009) reported that carbon gain was improved by fog which alleviated leaf water deficit, and addressed that the effect of dew/fog on net ecosystem exchange can vary by the duration of canopy wetting and the wettability of the leaf surface. However, it remains to be shown whether dew alleviates negative effects of a combined heat-drought on plant water status and ecosystem carbon exchange of grasslands, and which of the above mechanisms might dominate such a response.

Leaf water isotope signatures ($\delta^{18}\text{O}$ and $\delta^2\text{H}$) are useful to assess this question because they are natural tracers that can be used to assess plant physiological responses to environmental conditions (Bachmann et al., 2015; Prechsl et al., 2015). Evapotranspiration causes ^{18}O enrichment in leaf water compared to the source water (Dongmann et al., 1974; Farquhar and Lloyd, 1993). The magnitude of leaf water ^{18}O enrichment is strongly affected by the isotope signal of water vapor (Cernusak et al., 2002) and dew/fog (Kim and Lee, 2011; Goldsmith et al., 2017; Gerlein-Safdi et al., 2018), but also affected by foliar transpiration rates (Gessler et al., 2013). Typically, the leaf water ^{18}O signal is transferred onto leaf sugars *via* photosynthetic processes during daytime (Brandes et al., 2006; Gessler et al., 2013), and *via* the non-photosynthetic oxygen isotope exchange between leaf water and carbonyl groups of sugars (Wang et al., 2021). Leaf sugars are typically more enriched in ^{18}O compared to the leaf water due to the isotopic fractionation occurring during carbonyl hydration (Yakir and Deniro, 1990). Chamber experiments also suggested the transfer of the isotope signal of dew/fog on leaf water isotope signal during light and dark conditions (Kim and Lee, 2011; Gerlein-Safdi et al., 2018; Lehmann et al., 2020), and on leaf sugars during daytime conditions (Lehmann et al., 2020). However, it is not clear how large the photosynthetic and non-photosynthetic isotope imprints of leaf water on sugars are during nighttime as well as under low light and temperature conditions in the field.

Therefore, the main goals of this study focus on these three aims:

- 1) Quantify the combined effects of heat-drought stress and dew on net ecosystem production (NEP) by comparing the NEP before and during the heatwave, and analyzing leaf water-sugar isotope exchange in a chamber tracer experiment.
- 2) Quantify the combined effect of heat-drought stress and dew on plant water status by physiological and water isotope measurements.
- 3) Identify controls of atmospheric and soil conditions on plant water *via* analyzing the correlations of environmental variables with plant physiological and isotopic indicators.

We addressed these three aims using field data collected at an alpine grassland before and during the June 2019 heatwave, when a combined daytime heat-drought stress for the vegetation occurred during the day and dew formed during the night. H₂O vapor and net ecosystem CO₂ exchange were measured with the eddy-

covariance (EC) technique to assess the effects of these environmental conditions on the vegetation at the ecosystem scale. Physiological and water isotope measurements were employed to analyze the response of vegetation to these environmental conditions at plant scales.

2 Materials and methods

2.1 Study site

The Alp Weissenstein research site (CH-AWS, at 2000 m.a.s.l.) is part of a managed (grazed) alpine grassland ranging from 1900 to 2500 m.a.s.l. The vegetation composition was classified as *Deschampsia cespitosae*–*Poetum alpinae* community with red fescue (*Festuca rubra*), Alpine cat's tail (*Phleum rhaeticum*), white clover (*Trifolium repens*) and dandelion (*Taraxacum officinale*) as dominant species (Keller, 2006), complemented by alpine meadow-grass (*Poa alpina*) and lady's mantle (*Alchemilla vulgaris*). The soil types are slightly humous to humous sandy loam (Hiller et al., 2008), hence the permanent wilting point is estimated at around $0.1 \text{ m}^3 \text{ m}^{-3}$. The mean annual air temperature and precipitation were $1.9 \text{ }^\circ\text{C}$ (2015–2020; measured all year round at the site between 2015 and 2020; before 2015, data were only collected between May and October at the site) and 1213 mm (2013–2020; measured all year round between 2013 and 2020; before 2012, only the liquid precipitation was measured at the site), respectively. During the main growing season (May to September), monthly mean air temperatures were between $5.0 \text{ }^\circ\text{C}$ and $10.8 \text{ }^\circ\text{C}$ (2006–2018) with July as the hottest month (Figure 1A), while average monthly precipitation ranged from 87 to 128 mm (Figure 1B). During the growing season in 2019, the monthly

temperature ranged from $0.8 \text{ }^\circ\text{C}$ to $11.7 \text{ }^\circ\text{C}$ with June as the hottest month (Figure 1A), whilst the monthly precipitation ranged from 61 mm to 173 mm (Figure 1B).

2.2 Eddy covariance and meteorological measurements

EC measurements for H_2O vapor and net ecosystem CO_2 exchange have been carried out during the growing season since 2006 (tower coordinates: $46^\circ34'59.5'' \text{ N}$, $9^\circ47'25.5'' \text{ E}$ at 1978 m.a.s.l.). In mid-November 2014, the site was equipped with mains power for year-round operation. The EC instruments at CH-AWS in 2019 consisted of a three-dimensional sonic anemometer (model HS-50, Gill Instruments, Solent, UK) and an enclosed-path infrared gas analyzer (IRGA; Li-7200, Li-Cor, Lincoln, NB, USA), installed at 1.4 m agl (above ground level). EC measurements were recorded at 20 Hz and processed to 30 min averages using the EddyPro software Version 7.0.6 (LI-COR, 2019) following established community guidelines (Aubinet et al., 2012) for H_2O ($F_{\text{H}_2\text{O}}$ in $\text{mmol m}^{-2} \text{ s}^{-1}$) and CO_2 fluxes (F_{CO_2} in $\mu\text{mol m}^{-2} \text{ s}^{-1}$; net ecosystem exchange NEE). The micro-meteorological sign convention was used, with negative values denoting a downward flux, while positive values stand for upward fluxes. See details of footprint analysis of eddy-covariance measurements in Zeeman et al. (2010). Vapor pressure deficit (VPD) was quantified for 30-min intervals from ancillary air temperature and relative humidity measurements at 1.4 m agl (HygroClip HC2, Rotronic, Bassersdorf, Switzerland). Photosynthetic photon flux density (PPFD in $\mu\text{mol m}^{-2} \text{ s}^{-1}$) was measured at 1.3 m agl every 10 s (PARlite, Kipp & Zonen B.V., Delft, The Netherlands) and then averaged to 30-min

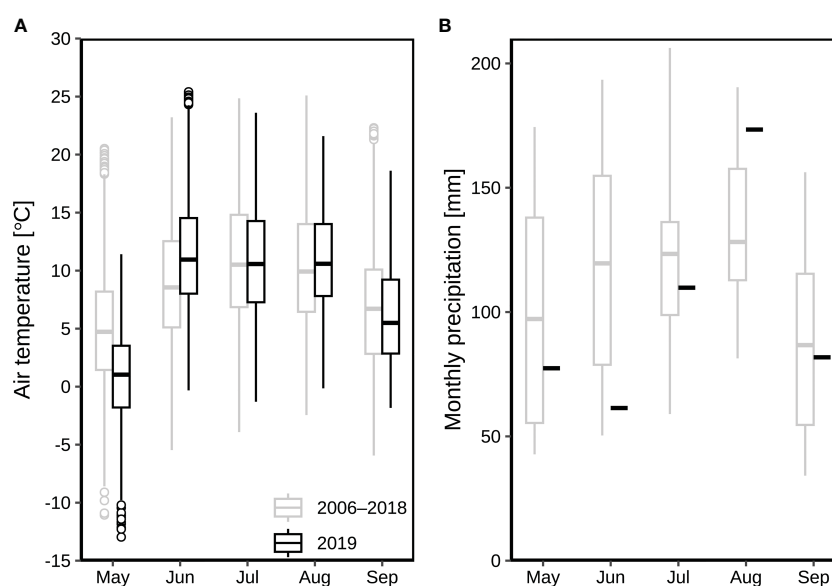


FIGURE 1

Air temperature and precipitation at the alpine grassland site CH-AWS in 2019 as compared to the period 2006–2018 (all data collected at the site): (A) average monthly air temperatures from May to September; (B) monthly precipitation from May to September. The boxplots show the medians, 25, and 75 quantile values (the inter-quartile range, IQR), with whiskers showing the data range up to 1.5 times the IQR. Values outside that range are shown with symbols.

intervals. Volumetric soil water content (SWC) was measured by two sensors (EC-5, Decagon Devices, Inc., Pullman, WA, USA) at 5 cm depth. NEP was calculated with the opposite sign of NEE (NEP = -NEE).

Diurnal NEP (g C m^{-2}) was calculated from the CO_2 flux (F_{CO_2}):

$$\text{NEP} = \sum(a \cdot t \cdot F_{\text{CO}_2} \cdot M_{\text{C}}) \quad (1)$$

where M_{C} is the molar mass of carbon (12 g C mol^{-1}), t is measurement intervals (1800 s) of F_{CO_2} , and a is a unit conversion factor ($10^{-6} \text{ mol } \mu\text{mol}^{-1}$).

For a long-term data series of air temperature at standard 2 m agl, an additional meteorological measurement setup was operating since 2006, installed at about 1180 m distance to the east and at approximately 40 m higher elevation compared to the flux tower (Michna et al., 2013). This additional setup provided air temperature (T_{a}) at 2 m agl (shaded, sheltered HydroClip S3, Rotronic AG, Basserdorf, Switzerland), and precipitation from an unheated pluviometer (LC, Texas Electronics, Dallas, USA). In November 2012, a precipitation gauge (1518H3, LAMBRECHT meteo GmbH, Göttingen, Germany) with a heatable orifice was installed between these two measurement stations (Michna et al., 2013) and provided annual total precipitation, including snowfall. Leaf wetness data were averaged from the measurements of two leaf wetness sensors (BNS, G. Luftt Mess-und Regeltechnik GmbH, Fellbach, Germany) installed since 2005 at 0.1 m agl close to the grassland canopy, using blotting paper inside a clip holder. The leaf wetness data was recorded by the voltage signal resulting from a fixed current applied from the center to the rim of the blotting paper. When the paper got wet by dew, fog, or rain, the blotting paper became conductive, and an increase in voltage signal was observed. We note that the leaf wetness sensors overestimated the leaf wetting duration (Figure S2), because the blotting paper dries out slower than the vegetation. By comparing the BNS sensor with a more accurate leaf wetness sensor (PHYTOS 31, Meter Group AG, Munich, Germany) at a later time of our observation campaigns (5–6 July 2020), the termination of leaf wetting was defined as the point when leaf wetness by BNS steeply and linearly decreased (Figure S2).

All variables were aggregated to 30 min averages or sums. The time series was recorded in CET (UTC+1 hour).

The evapotranspiration rate (ET in mm h^{-1}) was calculated from the H_2O flux ($F_{\text{H}_2\text{O}}$) as (Stull, 1988):

$$\text{ET} = b \cdot F_{\text{H}_2\text{O}} \cdot M_{\text{H}_2\text{O}} \quad (2)$$

where $M_{\text{H}_2\text{O}}$ is the molar mass of H_2O (18 g mol^{-1}), and b is a unit conversion factor [$= (10^{-3} \text{ mol mmol}^{-1}) \cdot (10^{-6} \text{ m}^3 \text{ g}^{-1}) \cdot (3600 \text{ s h}^{-1}) \cdot (10^3 \text{ mm m}^{-1}) = 0.0036 \text{ mol m}^2 \text{ s mm mmol}^{-1} \text{ g}^{-1} \text{ h}^{-1}$].

2.3 June 2019 heatwave and drought

According to our measurements at the CH-AWS site during 2006 to 2018, the hottest three months were typically June, July, and August, with average air temperatures (at standard 2 m agl) of 8.9, 10.8 and 10.3 °C (Figure 1A), respectively. As compared to the long-

term averages, the respective three months in 2019 were hotter with 11.7, 10.9, 10.8 °C (Figure 1A). The precipitation in June 2019 was 61 mm, which was only 51% of the long-term average of 120 mm in June during 2006–2018 (Figure 1B).

The 2019 heatwave occurred in Switzerland from 25 June to 1 July in 2019 (MeteoSwiss, 2019). No rain was recorded at the site from 23 June to 30 June 2019, but 0.2 mm rain was collected at 16:00 CET on 1 July 2019. Therefore, in this study, we only considered the 8-day rain-free period between 23 and 30 June 2019, with 23–24 June before the heatwave, and 25–30 June during the heatwave. Sunrise was around 04:30, and sunset was around 20:20 during the heatwave.

2.4 Experimental setup during measurement campaigns

To assess the combined effect of a well-developed natural drought during the heatwave in June 2019, we conducted two intensive measurement campaigns as intensive observation periods (IOP) at the end of the heatwave. These campaigns were carried out during two consecutive dew nights on 28–29 (IOP1 from 12:00 to 12:00 the next day) and on 29–30 (IOP2) June 2019.

2.4.1 Destructive sampling for isotope composition of water samples

To measure the isotope composition ($\delta^{18}\text{O}$ and $\delta^2\text{H}$) of leaf water, xylem water of root crowns, soil water, and dew droplets on leaf surfaces, destructive sampling was carried out during the IOP within 1 h before sunset (19:30 of IOP1 and IOP2), during the night (00:00 and 03:00 of IOP1 and IOP2), and after sunrise (06:00 of IOP1). Bulk leaf samples were taken in triplicates from randomly selected plants of four genera within an area of $70 \times 20 \text{ m}^2$, i.e., *Alchemilla* with palmately-lobed and hairy leaves, as well as toothed leaf edges; *Poa* with long and narrow grass leaves; *Taraxacum* with a rosette of long and wide jagged leaves; and *Trifolium* with obovate leaves (Figure S1). The average vegetation height was around 20 cm during our field campaigns. Root crown xylem samples were taken in triplicates after removing the attached soil and debris from randomly selected plants for each genus. Dew droplets were absorbed with cotton balls in six replicates from randomly selected plants. Soil cores were taken with a soil auger in triplicates and were then cut into slabs to separate four soil depths of 0–5 cm, 5–10 cm, 10–15 cm, and 15–20 cm. Leaf samples were taken at 19:30, 00:00, 03:00 and 06:00 during IOP1, as well as at 19:30, 00:00 and 03:00 during IOP2. Root crown samples were taken at 19:30, 00:00 and 03:00 during IOP1 and IOP2. Dew droplets were taken at 03:00 during IOP1 (no dew droplets were observed at 00:00), as well as at 00:00 and 03:00 during IOP2. The 0–5 cm soil samples were taken at 19:30, 00:00 and 03:00 during IOP1 and IOP2, while soil samples of 5–10 cm, 10–15 cm and 15–20 cm depth were taken at 19:30 and 03:00 during IOP1 and IOP2.

All samples were immediately transferred into glass tubes (Labco Exetainer® 12 ml Vial, Labco Ltd., Lampeter, UK), sealed

with caps and parafilm, and stored in a portable freezing box filled with dry ice blocks. Samples were then taken back to the laboratory and stored at -19°C . Dew water from cotton balls, and water from all plant and soil samples were extracted using a cryogenic vacuum extraction system (Prechsl et al., 2015). Using the high-temperature carbon reduction method (Werner and Brand, 2001; Gehre et al., 2004), the isotope composition of the respective water samples was determined by an isotope ratio mass spectrometer (IRMS, DeltaplusXP, Finnigan MAT, Bremen, Germany) coupling with a high-temperature conversion elemental analyzer (TC/EA, Finnigan MAT, Bremen, Germany) via a ConFlo III reference unit (Finnigan MAT, Bremen, Germany). The precision of $\delta^{18}\text{O}$ and $\delta^2\text{H}$ measurements for all the samples was $\pm 0.3\text{‰}$ and $\pm 0.7\text{‰}$, respectively. All isotope values of this study are expressed in the delta notation $\delta = (R_{\text{sample}}/R_{\text{standard}} - 1)$ in per mil (‰), where R_{standard} and R_{sample} are the molar ratios of either $^2\text{H}/^1\text{H}$ or $^{18}\text{O}/^{16}\text{O}$ of the standard (Vienna Standard Mean Ocean Water, V-SMOW) and the sample (IAEA, 2009; Coplen, 2011).

2.4.2 Isotope composition of atmospheric water vapor

The atmospheric water vapor at around 1 m agl was collected during IOP2 from 20:30 to 23:30, and from 00:00 to 03:00. Atmospheric air was pulled through a U-shaped glass tube that was placed in a Dewar filled with a cold slurry of ethanol and dry ice. After 3 h, the trapped water vapor frozen to the inner walls of the U-shaped glass tube was thawed, and the liquid water was filtered (Syringe filter, PTFE-Hydrophobic, $0.45\mu\text{m}$) and transferred into glass vials. The samples were measured with the TC/EA-IRMS for their isotope composition ($\delta^{18}\text{O}_{\text{vapor}}$ and $\delta^2\text{H}_{\text{vapor}}$) as described above. To compare the isotope composition of atmospheric water vapor with the liquid water pools (i.e., dew droplets, leaf water, xylem water of root crowns, and soil water), the isotope composition of the liquid ($\delta^{18}\text{O}_{\text{eq}}$ and $\delta^2\text{H}_{\text{eq}}$) in equilibrium with this vapor was calculated under the corresponding air temperature measured at 1.4 m agl following Horita and Wesolowski (1994).

2.4.3 Leaf water potential

To investigate the mechanism of dew influence on ecosystem water and carbon exchanges, leaf water status was measured at the end of the heatwave during our intensive observation campaigns (IOP1 and IOP2). The comparison of LWP before and after 29 June heatwave as well as two dew nights (the 28–29 and 29–30 nights) allows to compare the influence of heatwave and dew on leaf water status.

Leaf water potential (LWP) of the four genera *Alchemilla*, *Poa*, *Taraxacum*, and *Trifolium* was measured in triplicates with a Scholander pressure chamber (Model 1505D, PMS Instruments Co., Albany, OR, USA) using a grass compression gland for *Poa* and *Taraxacum*, and a round compression gland for *Alchemilla* and *Trifolium*. The LWP was measured within 1 h before sunset (19:30; before-sunset) and 2 h before sunrise (03:00; predawn) during IOP1 and IOP2.

2.4.4 Complementary *in-situ* chamber tracer experiment

Complementary to the sampling campaigns under natural conditions, an *in-situ* chamber tracer experiment was carried out during IOP1 (28–29 June) to investigate whether dew signal was used for carbon assimilation by determining the $\delta^{18}\text{O}$ and $\delta^2\text{H}$ values of leaf water and sugars. Within around 1 h before sunset, a $50 \times 50 \text{ cm}^2$ grassland plot was marked for the chamber tracer experiment. We used liquid water depleted in ^{18}O and ^2H as tracer ($\delta^{18}\text{O} = -364.7 \pm 1.9\text{‰}$ and $\delta^2\text{H} = -775.0 \pm 0.3\text{‰}$) and homogeneously sprayed it onto the plot at around 19:30. After spraying, the vegetation was immediately covered with a custom-made canopy chamber ($50 \times 50 \times 50 \text{ cm}^3$) wrapped with 0.1 mm thick polyethylene film, with a 76% transmissivity for thermal (longwave) infrared radiation (Horiguchi et al., 1982). With this tracer addition, we simulated dew, which was much more depleted in ^{18}O and ^2H than natural dew droplets. We note that we did not isolate the soil during the tracer amending on the grassland plot, hence the tracer could drip into the soil, and the amended tracer on vegetation can also drip to the soil, both of which can occur during natural dew formation processes. The canopy chamber did not fully isolate the grassland from the surrounding; thus, gas emission could still occur from the bottom rim of the chamber. But the chamber sufficiently suppressed the water vapor exchange between the within-chamber air and the open atmosphere. About 2 h before (03:00; predawn) and after sunrise (06:00), bulk leaf samples were taken in triplicates from randomly selected plants per genus in the plot. In addition, bulk leaf samples taken before sunset (19:30) acted as control for this experiment. Leaf water was extracted for isotope analyses ($\delta^{18}\text{O}_{\text{lw}}$ and $\delta^2\text{H}_{\text{lw}}$) as described in Section 2.3.1.

Leaf dry matter after cryogenic water extraction was milled to fine powder for $\delta^{18}\text{O}_{\text{ls}}$ and $\delta^{13}\text{C}_{\text{ls}}$ analysis of leaf sugars. Bulk sugars were extracted from 60 mg of this leaf powder with 1.5 mL deionized water at 85°C for 30 min (Lehmann et al., 2020). The neutral sugar fraction (defined here as “sugars”) was then further purified from ionic and phenolic substances by ion-exchange cartridges (OnGuard II A, H and P, Dionex; Thermo-Fisher Scientific, Bremen, Germany) following the protocol by Rinne et al. (2012). For the analysis of $\delta^{18}\text{O}_{\text{ls}}$, the purified bulk leaf sugars were filled into silver capsules, frozen and freeze-dried. The measurement precision (standard deviation) of the quality control standard (cellulose with 27.6‰ for $\delta^{18}\text{O}$) was $\leq 0.3\text{‰}$ for $\delta^{18}\text{O}_{\text{ls}}$ (Lehmann et al., 2018), and 0.1‰ for $\delta^{13}\text{C}_{\text{ls}}$ (Bögelein et al., 2019). $\delta^{13}\text{C}$ is the carbon isotope ratio in δ -notation in per mill (‰), relative to the international Vienna-Pee Dee Belemnite (V-PDB) standard, and were normalized by IAEA-CH7 (polyethylene, -32.2‰) and IAEA-CH3 (cellulose, -24.7‰) (Bögelein et al., 2019). Higher $\delta^{13}\text{C}_{\text{ls}}$ indicated lower water use efficiency (WUE) of plants.

In the chamber tracer experiment, the contribution of the tracer (f_{tracer}) to leaf water at 03:00 ($\delta^{18}\text{O}_{\text{lw},03:00}$) was simulated using a linear two-pool mixing model. One source of the leaf water was assumed to be the $\delta^{18}\text{O}_{\text{root}}$ at 03:00 of IOP1 ($\delta^{18}\text{O}_{\text{root},03:00}$) under natural conditions and the second source was the mean tracer $\delta^{18}\text{O}$ ($\delta^{18}\text{O}_{\text{tracer,mean}}$) taken up by the leaves during the night. We calculated $\delta^{18}\text{O}_{\text{tracer,mean}}$ as the mean of the original tracer $\delta^{18}\text{O}$

($\delta^{18}\text{O}_{\text{tracer}, 19:30} = -364.7 \pm 1.9\text{‰}$) and the $\delta^{18}\text{O}$ of the tracer which remained on the leaf surfaces by 03:00 ($\delta^{18}\text{O}_{\text{tracer}, 03:00}$ measured by absorbing the remaining tracer in form of simulated dew from the leaf surfaces at 03:00). f_{tracer} was calculated as:

$$f_{\text{tracer}} = \frac{\delta^{18}\text{O}_{\text{lw}, 03:00} - \delta^{18}\text{O}_{\text{root}, 03:00}}{\delta^{18}\text{O}_{\text{tracer}, \text{mean}} - \delta^{18}\text{O}_{\text{root}, 03:00}} \quad (3)$$

Due to the chamber acting as a heat-trap, the within-chamber temperature should be slightly higher than the open-air temperature. This temperature difference might affect the leaf-air water vapor exchange, but was assumed to have minor effect on foliar water uptake of liquid-phase dew and water-sugar isotope exchange.

2.5 Statistics

Tukey's honest significance test was used to assess differences among averages over sampling times and genera by the R-function agricolae::HSD.test (Steel, 1997) and one-way ANOVA. Reported statistical significance represents $p < 0.05$ with capital letters indicating temporal differences, and lower-case letters denoting genera or soil-depth differences. The isotopic and LWP results were reported in mean and standard errors of mean (SEM). We note that differences of isotope composition are always reported in absolute terms in per mil (‰). Correlation coefficients of regressions of NEP with T_a , PPFD, and RH were analyzed before and during the heatwave, with “***”, “**”, “*”, and “ns” indicating $p < 0.001$, $p < 0.01$, $p < 0.05$, and $p \geq 0.05$, respectively. During IOP1 and IOP2 at the end of the heatwave, considering the individual variability of plants, median values of leaf water isotope ($\delta^{18}\text{O}_{\text{lw}}$) and LWP by species at each sampling time were used for analyzing their correlations with environmental conditions (RH, SWC, and $\delta^{18}\text{O}_{\text{soil}}$), with “***”, “**”, “*”, and “ns” indicating $p < 0.001$, $p < 0.01$, $p < 0.05$, and $p \geq 0.05$, respectively. All analyses were carried out with R version 4.1.2 (R Core Team, 2021).

3 Results

3.1 Diel environmental variability before and during the heatwave

The diurnal and nocturnal air temperature averaged 14.5 °C and 7.3 °C before the heatwave during 23–24 June, but was 20.1 °C and 11.2 °C on average during the heatwave from 25 to 30 June (Figure 2A). The highest temperature of 25.4 °C was observed on 26 June 2019 (15:30; Figure 2A), indicating the peak of the heatwave, followed by 27 June 2019, the second hottest day. H_2O fluxes varied from -0.3 to $13.7 \text{ mmol m}^{-2} \text{ s}^{-1}$ (Figure 2B), corresponding to 3.0–4.7 mm of diurnal ET before the heatwave, and 4.9–5.7 mm during the heatwave (Figure 3A). SWC decreased from 0.32 to $0.15 \text{ m}^3 \text{ m}^{-3}$ during this rain-free period from 23 to 30 June (Figure 2C). NEP varied from -22 to $21 \text{ } \mu\text{mol m}^{-2} \text{ s}^{-1}$ (Figure 2D). The daytime NEP was 4.2–6.3 g C m^{-2} before the heatwave, but ranged from 5.4 to -2.9 g C m^{-2} during the heatwave

(Figure 3B). Negative NEP (-2.9 g C m^{-2}) occurred on 27 June, the day after the hottest day (26 June). Highest VPD was 2.06 kPa and 2.65 kPa before and during the heatwave (Figure 2E), respectively. The leaf wetness levels indicated that dew occurred during each night of the rain-free period, being fully evaporated from vegetation surfaces after 07:30 of day (Figure 2F). With dew occurrence during each night of the rain-free period (23–30 June), the corresponding nocturnal VPD was as low as 0.14–1.41 kPa (Figure 2E).

3.2 Effects of heat-drought and dew on net ecosystem production

Before the heatwave, NEP almost linearly increased with PPFD (Figure 4), with higher diurnal NEP (6.3 g C m^{-2}) on 23 June than that on 24 June (4.2 g C m^{-2} ; Figure 3B). The suppression of heat-drought stress on NEP was substantial on the hottest day (26 June with 2.0 g C m^{-2}) during the heatwave (Figure 3B), with 63% of reduction in NEP compared to the previous day (25 June with 5.4 g C m^{-2} of NEP). Negative diurnal NEP (-2.9 g C m^{-2}) occurred on the second hottest day (27 June; Figure 3B), with longer period (09:00–15:00) of net carbon emission (negative NEP) under PPFD $> 1300 \text{ } \mu\text{mol m}^{-2} \text{ s}^{-1}$ and $T_a > 22.5 \text{ } ^\circ\text{C}$ (Figure 4E), as compared to the hottest day during 14:00–16:30 under PPFD $> 1800 \text{ } \mu\text{mol m}^{-2} \text{ s}^{-1}$ and $T_a > 25.3 \text{ } ^\circ\text{C}$ (Figure 4D). Daily NEP recovered to the levels of 4.7–5.0 g C m^{-2} on 28–30 June after the hottest two days on 26–27 June (Figure 3B).

During the early morning hours before 07:30 with leaf wetting by dew, NEP increased by T_a before and during the heatwave (Figure 5A; $p < 0.01$ and $p < 0.001$ before and during the heatwave, respectively), but the turning T_a from negative (net carbon emission) to positive (net carbon sequestration) NEP was higher during the heatwave period (13.7 °C for 25–30 June) than that before the heatwave (8.2 °C for 23–24 June). With vegetation wetting by dew in the early morning hours, NEP exponentially increased with PPFD ($p < 0.01$ and $p < 0.001$ before and during the heatwave, respectively), but NEP was lower during the heatwave than that before the heatwave under same levels of PPFD (Figure 5B). In the early morning hours with vegetation wetting, NEP slightly increased by leaf wetness levels before the heatwave (Figure 5C; $p \geq 0.05$), but significantly decreased by leaf wetness levels at the beginning of the heatwave on 25–26 June (Figure 5D; $p < 0.01$).

3.3 Effects of heat-drought and dew on leaf water status and leaf isotopes

3.3.1 Leaf water status

Comparing predawn (03:00) periods of IOP1 and IOP2 (Figure 6), *Poa* LWP significantly decreased from -0.9 to -1.5 MPa ($p < 0.05$), *Trifolium* LWP slightly decreased from -0.4 to -0.7 MPa ($p \geq 0.05$), *Taraxacum* LWP was at similar levels (-0.6 to -0.6 MPa ; $p \geq 0.05$), whilst *Alchemilla* LWP slightly increased from -0.7 to -0.3 MPa ($p \geq 0.05$). Comparing before-sunset (19:30) periods of IOP1 and IOP2 (Figure 6), *Poa* LWP

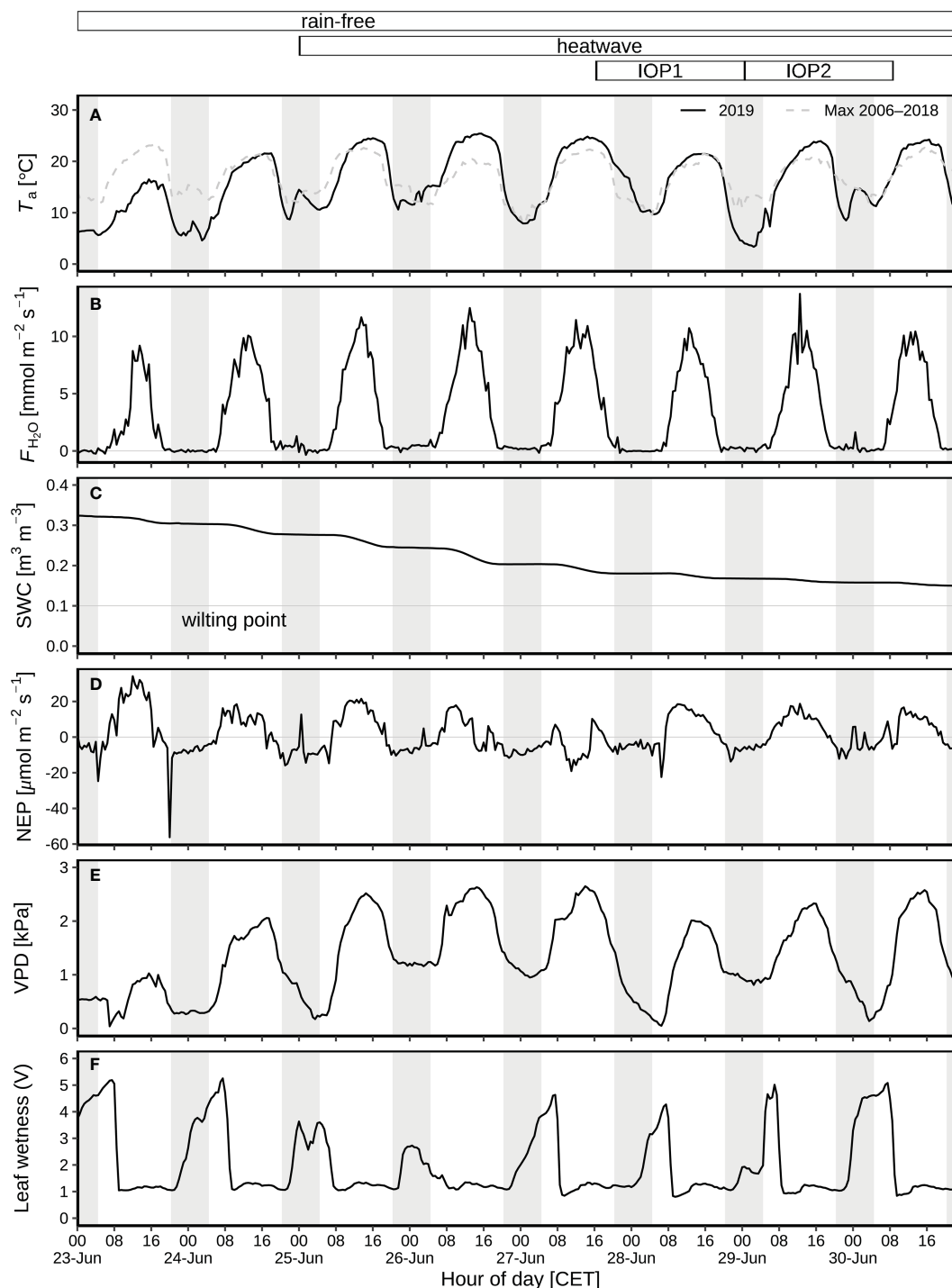


FIGURE 2

Environmental variables during the rain-free period (23–30 June) at CH-AWS site before the heatwave on 23–24 June, and during the June 2019 heatwave on 25–30 June: (A) air temperature (T_a) at 2 m agl as compared to the long-term maximum 2006–2018. (B) Eddy-covariance H_2O flux. (C) Volumetric soil water content (SWC) at 5 cm depth. (D) Net ecosystem production (NEP); positive numbers indicate CO_2 emission, and negative numbers represent CO_2 uptake. (E) Vapor pressure deficit (VPD). (F) Leaf wetness recorded by the voltage signal resulting from a fixed current applied from the center to the rim of the blotting paper; substantial increase in leaf wetness during nighttime and early morning indicate leaf wetting by dew during the rain-free period; dew occurred on each night of the period. Field campaigns were carried out during two intensive observation periods (IOP) on 28–29 (IOP1) and 29–30 (IOP2) June 2019. Hours of day are given in CET. The grey shaded areas represent nocturnal periods.

significantly decreased from -0.9 to -1.8 MPa ($p < 0.05$), *Taraxacum* LWP (-1.1 to -1.1 MPa) was at similar levels, whilst *Trifolium* LWP slightly increased from -1.3 to -1.0 MPa ($p \geq 0.05$) and *Alchemilla* LWP increased from -1.6 to -0.6 MPa ($p \geq 0.05$).

The LWP of all four genera slightly increased during both IOP nights ($p \geq 0.05$; Figure 6), i.e., from before-sunset (19:30) to pre-dawn periods (03:00). Among the four genera, *Alchemilla* had the lowest LWP before sunset of IOP1 ($p \geq 0.05$), but had slightly

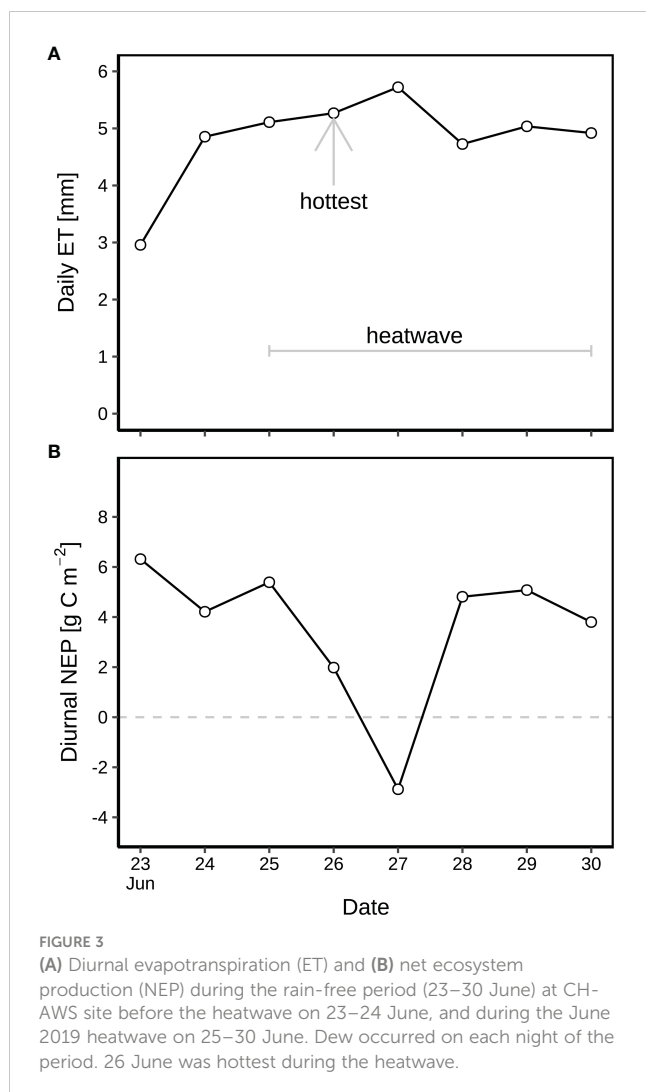


FIGURE 3
(A) Diurnal evapotranspiration (ET) and **(B)** net ecosystem production (NEP) during the rain-free period (23–30 June) at CH-AWS site before the heatwave on 23–24 June, and during the June 2019 heatwave on 25–30 June. Dew occurred on each night of the period. 26 June was hottest during the heatwave.

higher LWP than the other three genera before sunset of IOP2 ($p \geq 0.05$). On the contrary, *Poa* had slightly lower LWP than the other three genera at the predawn period of IOP1 ($p \geq 0.05$), but had much lower LWP than the other three genera at predawn of IOP2 ($p < 0.05$). Therefore, *Poa* LWP significantly decreased ($p < 0.05$) at the end of the heatwave, whilst *Alchemilla* LWP significantly increased ($p < 0.05$), *Taraxacum* and *Trifolium* slightly increased ($p \geq 0.05$) although heat-drought stress.

3.3.2 Isotope composition of different water pools at natural isotope abundances

The $\delta^{18}\text{O}_{\text{soil}}$ ($-9.5 \pm 1.6\text{‰}$; Figure 7A) varied with depth ($p < 0.05$), with higher $\delta^{18}\text{O}_{\text{soil}}$ ($-8.1 \pm 1.4\text{‰}$) in top soil layer (0–5 cm depth) and lower $\delta^{18}\text{O}_{\text{soil}}$ ($-10.2 \pm 1.2\text{‰}$) in subsoil layers (5–20 cm depth). $\delta^{18}\text{O}_{\text{root}}$ was within the range of $\delta^{18}\text{O}_{\text{soil}}$ (Figures 7A, B), indicating soil water as the main source of plant water. $\delta^{18}\text{O}_{\text{root}}$ of *Alchemilla* and *Trifolium* was between the topsoil and the subsoil $\delta^{18}\text{O}_{\text{soil}}$, whilst $\delta^{18}\text{O}_{\text{root}}$ of *Poa* and *Taraxacum* was close to subsoil $\delta^{18}\text{O}_{\text{soil}}$. $\delta^{18}\text{O}_{\text{root}}$ varied with plant genera ($p < 0.05$; Figure 7B), with higher $\delta^{18}\text{O}_{\text{root}}$ for *Alchemilla* and *Trifolium* ($-9.0 \pm 1.0\text{‰}$), but lower $\delta^{18}\text{O}_{\text{root}}$ for *Poa* and *Taraxacum* ($-10.6 \pm 1.0\text{‰}$). The

comparison of $\delta^{18}\text{O}_{\text{soil}}$ and $\delta^{18}\text{O}_{\text{root}}$ (Figure 7B) indicated that *Alchemilla* and *Trifolium* used shallower soil water as compared to *Poa* and *Taraxacum*.

Across all four genera, leaf water $\delta^{18}\text{O}_{\text{lw}}$ ($-2.6 \pm 4.8\text{‰}$; Figure 7C) was on average higher than $\delta^{18}\text{O}_{\text{root}}$ ($-9.8 \pm 1.3\text{‰}$; Figure 7B), indicating evaporative processes of leaf water as compared to xylem water. *Poa* had the highest $\delta^{18}\text{O}_{\text{lw}}$ among the four genera ($p < 0.05$; Figure 7C), indicating strongest water stress of *Poa* derived from their stronger evaporation or stress-induced partial stomatal closure. *Taraxacum* tended to have the lowest $\delta^{18}\text{O}_{\text{lw}}$, but not significantly different from *Alchemilla* and *Trifolium* ($p \geq 0.05$). $\delta^{18}\text{O}_{\text{dew}}$ changed over time, with $-7.5 \pm 0.4\text{‰}$ at 03:00 of IOP1, increasing to $-6.7 \pm 1.0\text{‰}$ at 00:00 and $-5.7 \pm 0.5\text{‰}$ at 03:00 during IOP2 ($p \geq 0.05$; Figure 7B). $\delta^{18}\text{O}_{\text{eq}}$ of the liquid water in equilibrium with atmospheric water vapor was -5.0‰ to -4.7‰ during 20:30 to 03:00 of IOP2. Compared to the local meteoric water line (LMWL; $\delta^2\text{H} = 7.83 \delta^{18}\text{O} + 12.97$; following Prechsl et al., 2014), $\delta^2\text{H}_{\text{eq}} - \delta^{18}\text{O}_{\text{eq}}$ was above the LMWL. In contrast, all $\delta^2\text{H} - \delta^{18}\text{O}$ pairs for dew droplets, plants and soil water fell below the LMWL, indicating evaporation of these water pools compared to local precipitation, particularly of leaf water (Figure 7D).

3.3.3 Effect of isotopically labelled dew on leaf water and sugar isotopes

Adding isotopically ^{18}O -depleted water as a tracer in the chamber tracer experiment on IOP1 night induced a substantial ^{18}O -depletion in leaf water ($\delta^{18}\text{O}_{\text{lw}}$; $p < 0.05$), but not so in leaf sugars ($\delta^{18}\text{O}_{\text{ls}}$; $p \geq 0.05$; Figure 8A). Before applying the tracer at 19:30 (before sunset), $\delta^{18}\text{O}$ of leaf sugar ($\delta^{18}\text{O}_{\text{ls}}$) for the four genera ($29.9 \pm 2.9\text{‰}$; Figure 8A) was 30.1‰ higher than their respective $\delta^{18}\text{O}_{\text{lw}}$ ($-0.2 \pm 3.4\text{‰}$). During the following 7.5 h overnight (until 03:00), $\delta^{18}\text{O}_{\text{lw}}$ of the four genera decreased by a further $26.6 \pm 10.4\text{‰}$ as compared to before-sunset levels. In contrast, $\delta^{18}\text{O}_{\text{ls}}$ ($29.2 \pm 4.5\text{‰}$) of the four genera did not change after tracer amendment, and consequently $\delta^{18}\text{O}_{\text{ls}}$ of the four genera was 55.7‰ higher than the respective $\delta^{18}\text{O}_{\text{lw}}$ (Figure 8A). Wet foliage due to tracer application persisted for 10.5 h, thus after sunrise (06:00), $\delta^{18}\text{O}_{\text{lw}}$ of the four genera increased to $-14.6 \pm 4.7\text{‰}$ in respect to predawn $\delta^{18}\text{O}_{\text{lw}}$, whereas the corresponding $\delta^{18}\text{O}_{\text{ls}}$ ($26.3 \pm 1.3\text{‰}$) remained almost constant over the night until sunrise, indicating minor effect of amended tracer on soil moisture. As a result, $\delta^{18}\text{O}_{\text{ls}}$ of the four genera after sunrise was 40.9‰ higher than the corresponding $\delta^{18}\text{O}_{\text{lw}}$ (Figure 8A).

The changes in $\delta^{18}\text{O}_{\text{lw}}$ varied by genus before and during the chamber tracer experiment. Before sunset and tracer amendment, *Poa* $\delta^{18}\text{O}_{\text{lw}}$ ($4.7 \pm 1.3\text{‰}$) was 6.6‰ higher than $\delta^{18}\text{O}_{\text{lw}}$ of the other three genera ($-1.9 \pm 1.8\text{‰}$; Figure 8A), indicating more severe water stress of *Poa*. However, the difference for predawn (03:00) $\delta^{18}\text{O}_{\text{lw}}$ of *Poa* ($-15.4 \pm 2.8\text{‰}$; Figure 8A) increased to 15.3‰ compared to the corresponding $\delta^{18}\text{O}_{\text{lw}}$ of the other three genera ($-30.7 \pm 8.9\text{‰}$; Figure 8), which might be due to the stronger evaporation and less foliar water uptake of *Poa*, or stress-induced partial stomatal closure. Overall, the ranking of the genera stayed relatively stable, with *Poa* typically showing the highest $\delta^{18}\text{O}_{\text{lw}}$.

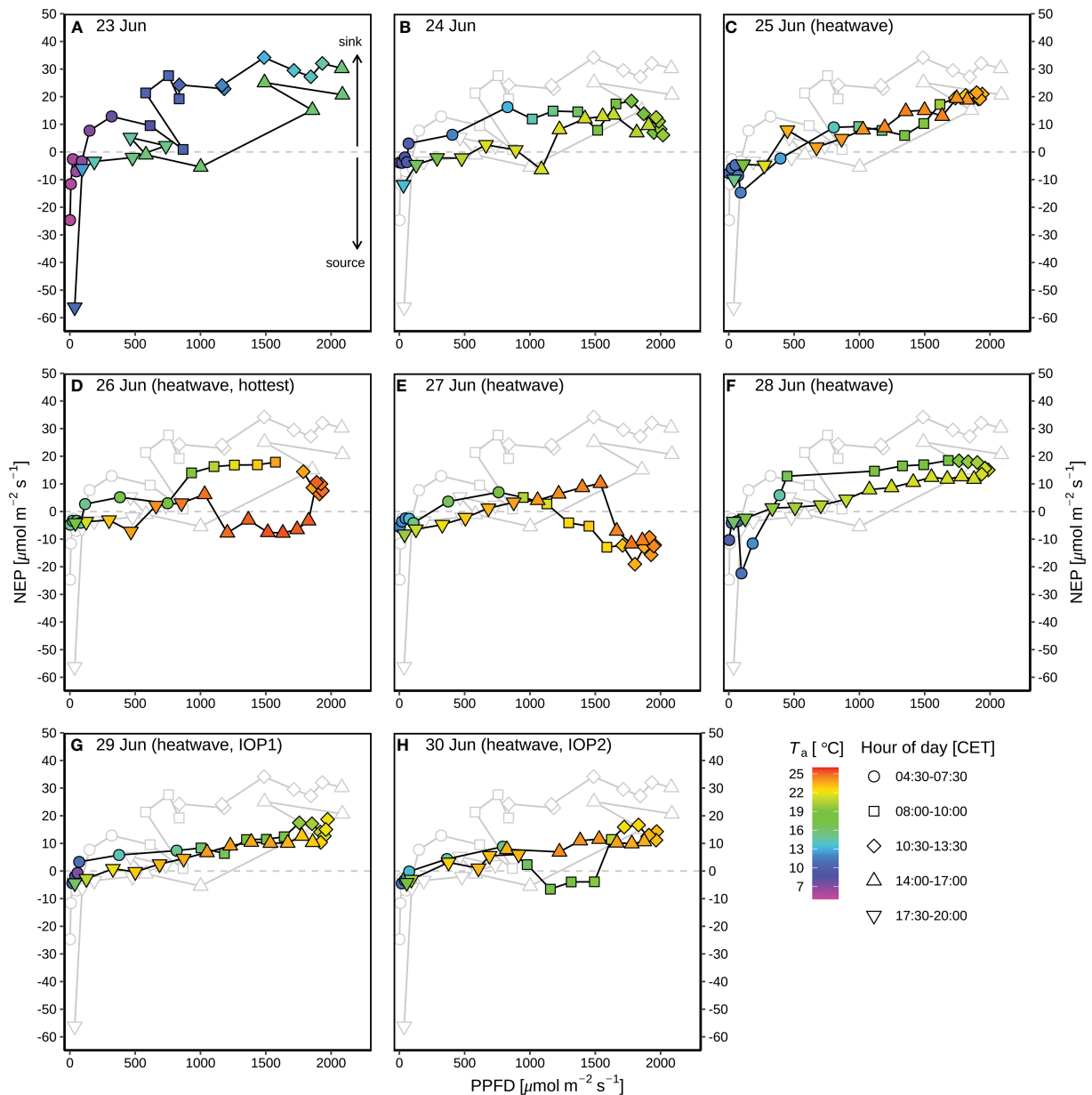


FIGURE 4

Response curves of diurnal net ecosystem production (NEP) to photosynthetic photon flux density (PPFD) during the rain-free period (23–30 June) at CH-AWS site before the heatwave on 23–24 June (A, B), and during the June 2019 heatwave on 25–30 June (C–H). Different hours of day (CET) are shown in different shapes; the colors of the symbols indicate the corresponding air temperature (T_a). Dew occurred during each night of the period. For comparison, the grey plots in panels (B–H) show the NEP-PPFD response curve on 23 June 2019 before the heatwave.

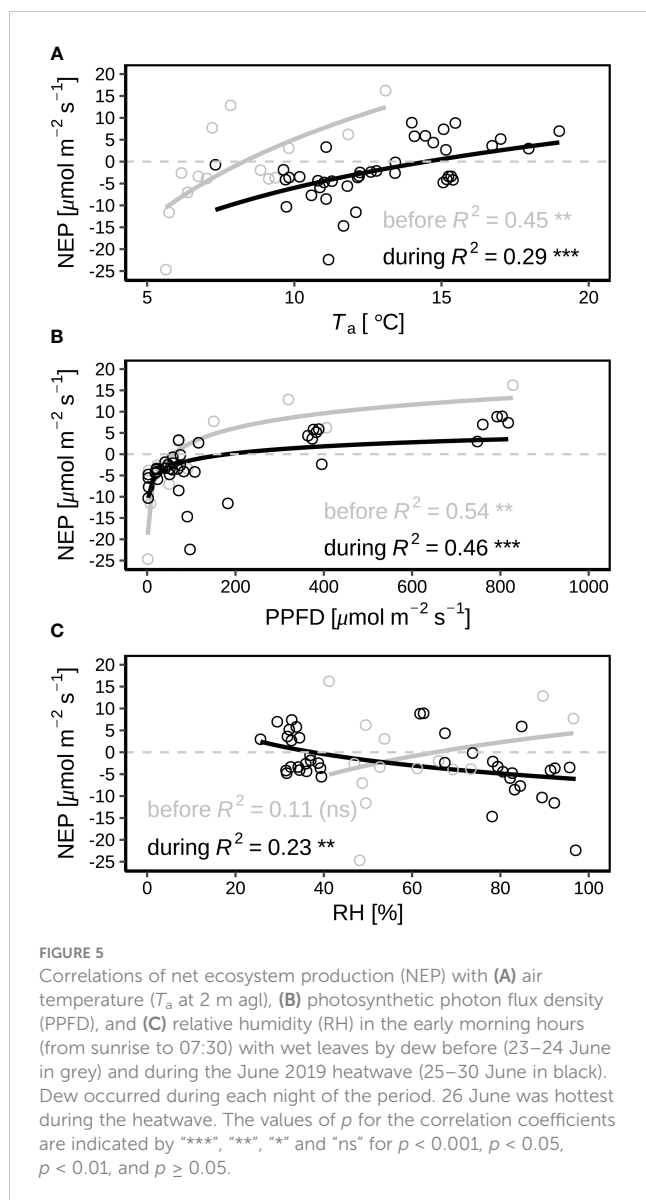
During the experiment, $\delta^{18}\text{O}$ of the added tracer increased from -364.7‰ at 19:30 to $-19.5 \pm 1.8\text{‰}$ at 03:00 (Figure 8C). The contribution (f_{tracer}) of the added tracer ($\delta^{18}\text{O}_{\text{tracer_mean}}$ of -192.1‰) to plant leaf water was 3–14%, highest for *Alchemilla* and lowest for *Poa* (Figure 8D). f_{tracer} was positively correlated with the corresponding predawn LWP, except for *Alchemilla* with large variability in their predawn LWP (Figure 8E).

$\delta^{13}\text{C}_{\text{ls}}$ was rather constant over the IOP1 night. Higher $\delta^{13}\text{C}_{\text{ls}}$ of *Alchemilla* and *Poa* indicated their lower WUE, as compared to *Taraxacum* and *Trifolium* (Figure 8B). $\delta^{13}\text{C}_{\text{ls}}$ of *Poa*, *Taraxacum* and *Trifolium* was negatively correlated with f_{tracer} (Figure 8F),

whilst *Alchemilla* with highest f_{tracer} showed highest $\delta^{13}\text{C}_{\text{ls}}$ and thus lowest WUE.

3.4 Controls of atmospheric and soil conditions on plant water

LWP of *Taraxacum* and *Trifolium* were positively correlated with RH (Figure 9A), indicating the controls of atmospheric humidity on their LWP. LWP of *Poa* was positively correlated with SWC (Figure 9B), indicating the controls of soil moisture on



their LWP. This corresponded to the significant decline of *Poa* LWP at the end of the heatwave (Figure 6), under the conditions of low SWC ($0.15 \text{ m}^3 \text{ m}^{-3}$; Figure 2C) close to wilting point. LWP and $\delta^{18}\text{O}_{\text{lw}}$ of *Alchemilla*, *Taraxacum* and *Trifolium* were negatively correlated (Figure 9C), indicating the controls of leaf water content on their $\delta^{18}\text{O}_{\text{lw}}$. Stronger drought-stress of *Poa* might induce partial stomatal closure, and thus result in their more enriched leaf water isotopes (higher $\delta^{18}\text{O}_{\text{lw}}$) not relevant to LWP. The slightly improved *Alchemilla* LWP at the end of the heatwave might be derived from the accumulated benefits by dew, which contributed more to *Alchemilla* leaf water (14%; Figure 8D) compared to the other three genera ($\leq 12\%$). $\delta^{18}\text{O}_{\text{lw}}$ of *Alchemilla*, and *Taraxacum* was negatively correlated with RH (Figure 9D), indicating the control of atmospheric conditions on their $\delta^{18}\text{O}_{\text{lw}}$. $\delta^{18}\text{O}_{\text{lw}}$ did not show significant correlation with SWC and $\delta^{18}\text{O}_{\text{soil}}$ (Figures 9E, F), indicating the minor control of soil water on leaf water isotopes.

4 Discussion

4.1 Dew benefits cancelled out by heat-drought stress

The benefits of dew on NEP were observed in the early morning hours of 23–24 June before the heatwave (Figure 10). From sunrise to 06:30 on 23 and 24 June, PPFD was at similar levels (Figure 10C), hence higher NEP on 24 June (Figure 10A) might be induced by higher temperature (Figure 10D) as compared to 23 June. But from 06:30 to 07:30, although higher PPFD and temperature on 24 June, NEP was at the similar levels as that on 23 June (Figure 10C), probably induced by higher potential of dew formation as indicated in higher RH on 23 June (Figure 10B).

However, with the occurrence of heatwave, dew benefits on NEP were cancelled out, as shown in the reduced NEP with increasing RH (Figure 5C). The chamber tracer experiment at the end of the heatwave showed that dew isotope signal was not transferred to leaf sugar (Figure 8A), indicating that dew water did not participate in carbon assimilation during the heatwave. The possible reason could be derived from the minor contribution (3–14%) of dew water to plant leaf water (Figure 8D), corresponding to previous research that foliar water uptake can only increase leaf water content by 2–11% (Limm et al., 2009). Due to the heat-drought stress, partial stomatal closure and vapor pressure gradient (Li et al., 2023) from leaf to atmosphere (saturated leaf internal environment vs unsaturated atmospheric conditions) might limit the uptake of dew water *via* leaf, thus most of the dew water during the heatwave could evaporate after sunrise instead of being used for carbon assimilation. Oliveira et al. (2021) showed that dew evaporation processes induced CO_2 loss of a maritime pine forest during the rain-free period after wildfire, but Simonin et al. (2009) reported that the reduction in leaf water deficit by fog water can result in improved carbon gain. Therefore, the effect of dew on ecosystem exchange varied by environmental conditions, e.g., environmental stress (Oliveira et al., 2021), the duration of canopy wetting (Simonin et al., 2009), the wettability of the leaf surface (Brewer and Smith, 1994; Hanba et al., 2004), and the foliar water uptake capacity of plants (Simonin et al., 2009).

Our tracer chamber experiment was carried out in a single chamber, and with only once sampling after sunrise, thus it was not possible to investigate the effect of dew on carbon assimilation after dew totally evaporating from surfaces. Future research on hourly resolution and longer period of after-sunrise isotope measurements is recommended to answer this question.

4.2 Ecosystem water and carbon exchange

Despite heat-drought stress, alpine grassland kept high ET during the heatwave (Figure 3A), as long as soil moisture was available (Figure 2C) to meet its evaporative demand (Teuling et al., 2010; Wolf et al., 2013).

De Boeck et al. (2016) showed that a combined heatwave and drought stress induced a reduction in above-ground biomass of

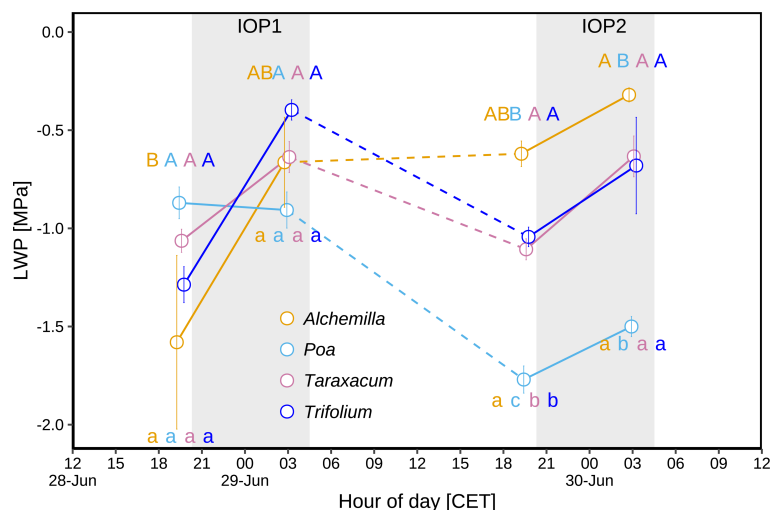


FIGURE 6

Leaf water potential (LWP) during two intensive observation periods (IOP1 and IOP2) with nocturnal dew occurrence at the end of the June 2019 heatwave: LWP of different plant genera (*Alchemilla*, *Poa*, *Taraxacum*, and *Trifolium*) were measured before sunset (at 19:30 within around 1 h before sunset) and before sunrise (03:00 within around 2 h before sunrise) of two dew events. Different letters indicate statistically significant differences ($p < 0.05$), with capital letters indicating temporal comparison, and lower cases indicating among-genera comparison. The grey shaded areas represent nocturnal periods.

alpine grassland plants. In this study, the reduction of NEP by the heat-drought stress was most pronounced during the two hottest days (26 and 27 June; Figures 4D, E) of the heatwave period. Compared to 26 June (25.4 °C; Figure 4B), 27 June showed a longer period of net carbon emission (Figure 4E) despite lower maximum T_a (24.8 °C; Figure 5E) and SWC (Figure 2C). This might be explained by an intensifying effect of drought stress, corresponding to previous research by De Boeck et al. (2016), and the influence of severe heat stress on nighttime refilling. Nevertheless, heat stress was a bit relieved after the heatwave peak, when temperatures only reached 21.5 °C, and NEP recovered immediately. The rapid re-growth ability of alpine plants after heat-drought stress (Brilli et al., 2011) might explain the recovery of NEP during 28–30 June (Figure 3B) after the hottest two days. This also corresponded to the fact that LWP of plants (except *Poa*) did not significantly decrease at the end of the heatwave (Figure 6). The refilling of plant tissues during the night is a well-known phenomenon (Schulze et al., 2019), helping to relieve water losses during heat-drought stress, and might contribute to the recovery of diurnal NEP on 28–30 June after the peak of the heatwave to the levels slightly lower than the beginning of the heatwave on 23–25 June. The redistribution of soil water by deeper plant roots to the shallower soil depths might provide sufficient soil moisture sources for plant tissue refilling (Burgess and Bleby, 2006) after the peak of the heatwave. This may also explain why the predawn LWP of *Alchemilla*, *Taraxacum*, and *Trifolium* did not decline at the end of the heatwave. Yet, the nighttime refilling mechanism of plant tissues might not always lead to a full recovery of NEP at daily scales, particularly in the case of extreme heat-drought stress. As a result, the most severe decline of NEP was observed during the peak of the heatwave on 26–27 June. The most severe heat stress on 26 June might cause the suppression of tissue refilling during the following night, and thus more

pronounced NEP reduction was observed on the next day (27 June) instead of on the hottest day (26 June). The decline of *Poa* LWP (Figure 6) might be due to their more severe drought stress (as indicated in their higher $\delta^{18}O_{lw}$ as compared to the other three genera; Figures 7A, 8A) and dependence on soil moisture (Figure 9B). The decline of *Poa* LWP had minor effect on NEP, probably due to their small plant size and stress-induced partial stomatal closure. We could not quantify the individual contribution of different genera on ecosystem water and carbon fluxes, and effect of eddy-covariance footprint; thus, we suggest that future research can combine ecosystem-scale eddy-covariance fluxes, footprint models and plant-scale chamber fluxes, complemented by plant community compositions to quantify the effect of different genera on ecosystem exchange.

Dew amount was found to be underestimated by eddy-covariance H_2O fluxes because dew occurs on clear and calm nights with stably stratified nocturnal boundary layer (Jacobs et al., 2006; Li et al., 2021). High accuracy weighing lysimeters can be an option to quantify dew amount into ecosystems (Riedl et al., 2022; Ucles et al., 2013). CO_2 fluxes can be measured by eddy-variance (Eugster and Siegrist, 2000) and laser (Maier et al., 2022) approaches. For alpine ecosystems, a challenge is the topographic variability that induces large uncertainties of CO_2 fluxes (Hammerle et al., 2007). Due to the low quality of CO_2 fluxes during nighttime by eddy-covariance measurements, we could not assess the dew effect in darkness. Furthermore, the benefits of dew on ecosystems can continue after dew drying out on vegetation surfaces, which could be traced by high-resolution measurements of H_2O and CO_2 isotopes, but was not possible in this study based on 3–13 h intervals of destructive isotope sampling. Therefore, additional methods, e.g., synchronized and continuous laser measurements of H_2O and CO_2 fluxes (Li et al., 2021; Maier et al., 2022) and their isotopic fluxes (Siegwolf et al., 2021) at both plant and ecosystem scales need to be

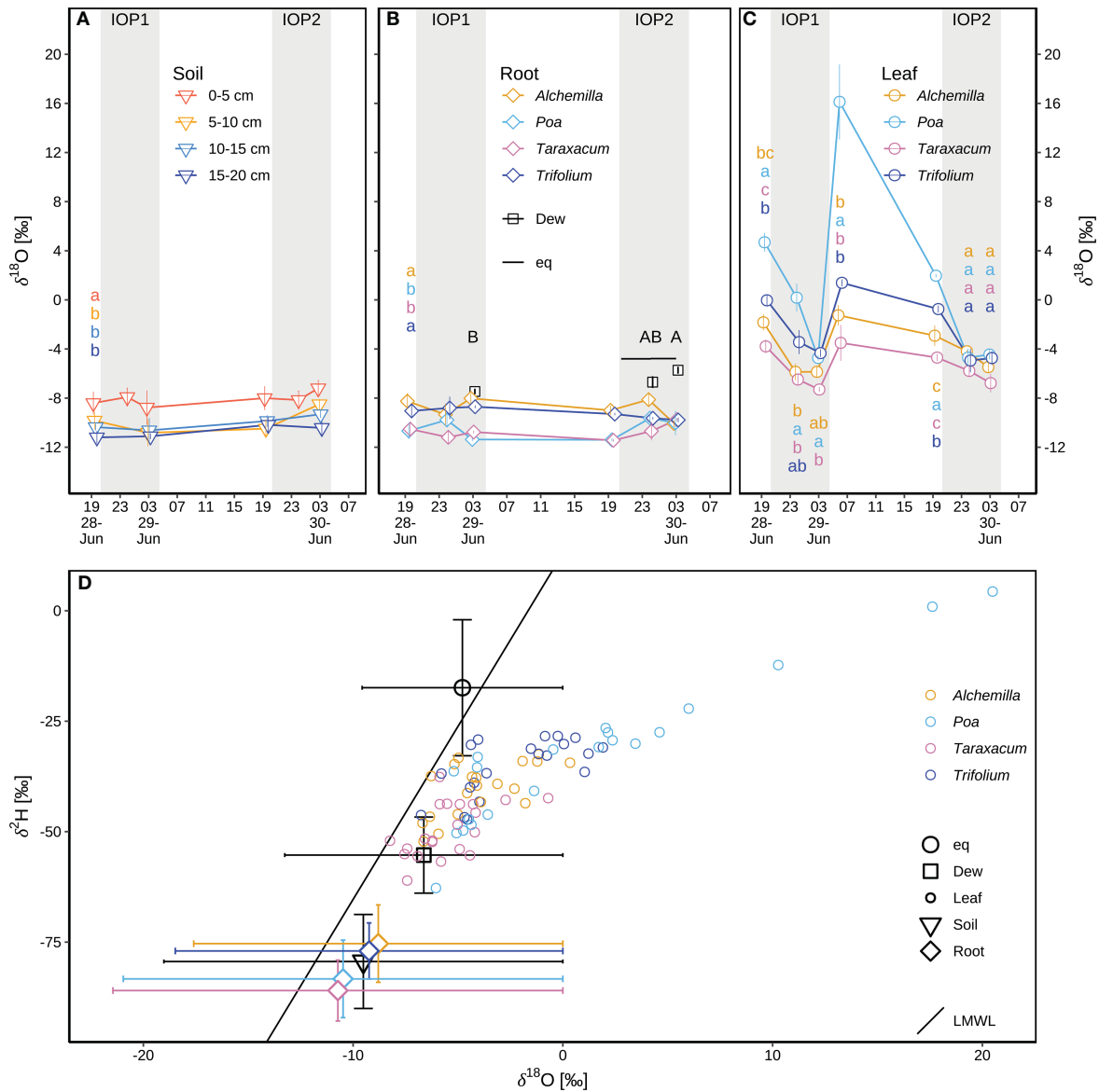


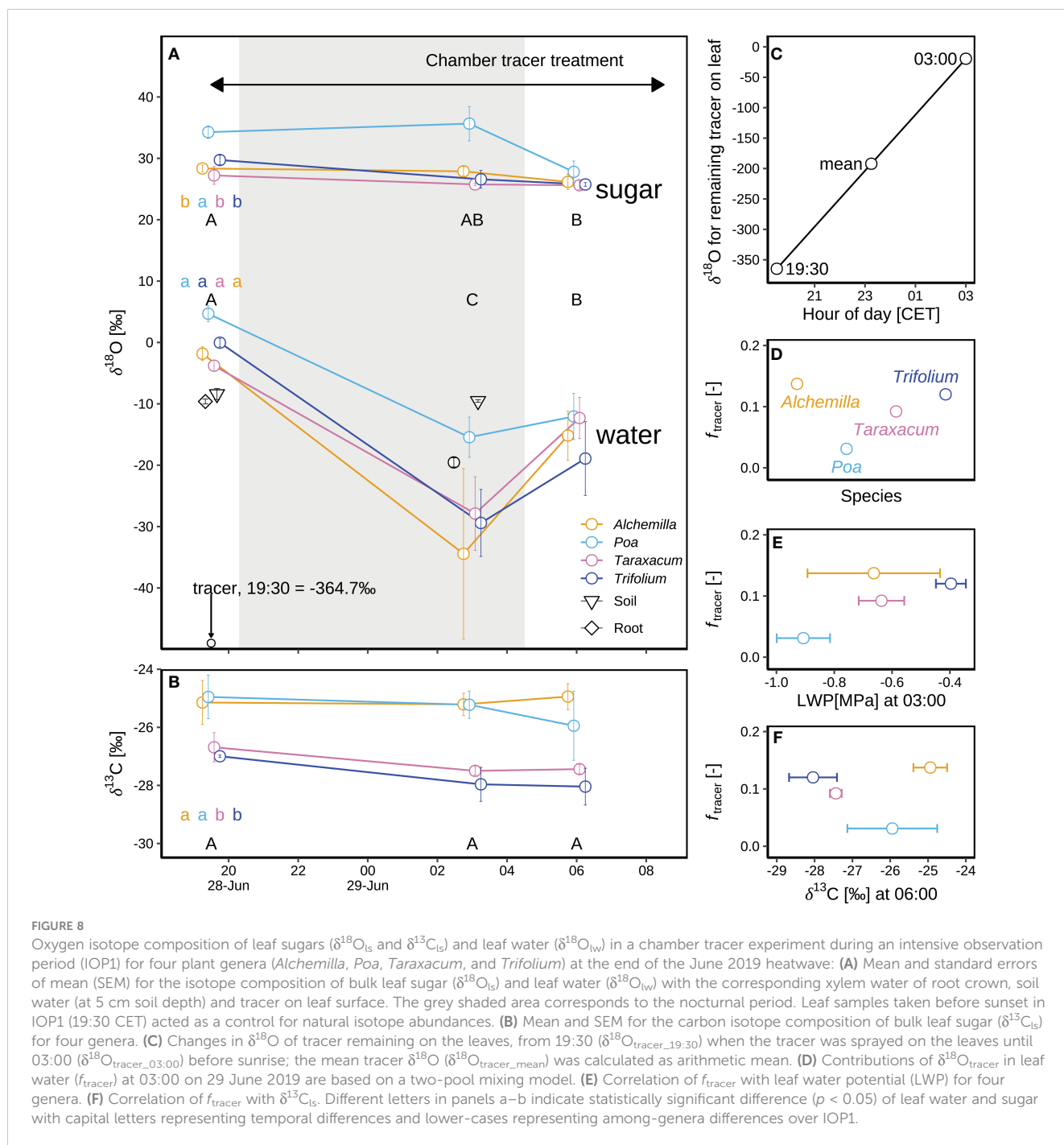
FIGURE 7 Isotope composition of different water pools during two consecutive intensive observation periods (IOP1 and IOP2) with nocturnal dew formation at the end of the June 2019 heatwave: **(A)** soil water $\delta^{18}O_{soil}$ at different depths (0–5, 5–10, 10–15, and 15–20 cm); different lower-case letters indicate statistical significance of among-soil-depth difference ($p < 0.05$) of $\delta^{18}O_{soil}$ over IOPs. **(B)** Dew droplets $\delta^{18}O_{dew}$ on plant surfaces; the liquid $\delta^{18}O_{eq}$ in equilibrium with atmospheric water vapor; xylem water of root crown $\delta^{18}O_{root}$ for four genera (*Alchemilla*, *Poa*, *Taraxacum*, *Trifolium*); different lower-case letters indicate statistical significance of among-genera difference ($p < 0.05$) of $\delta^{18}O_{root}$ over IOPs; different capital letters in black indicate statistical significance of among-sampling-time difference ($p < 0.05$) of $\delta^{18}O_{dew}$. **(C)** Leaf water $\delta^{18}O_{lw}$ for four genera; different lower-case letters indicate statistical significance of among-genera difference ($p < 0.05$) for $\delta^{18}O_{lw}$ at each sampling time. Mean and standard errors of mean (SEM) are shown in panels **(A–C)**. **(D)** $\delta^2H-\delta^{18}O$ pairs compared to the local meteoric water line (LMWL: $\delta^2H = 7.83\delta^{18}O + 12.97$) following [Prechtl et al. \(2014\)](#); $\delta^2H-\delta^{18}O$ of equilibrium liquid, dew samples, and soil samples was mean and SEM over IOPs; $\delta^2H-\delta^{18}O$ of xylem water of root crown was mean and SEM by species over IOPs; raw data of leaf water $\delta^2H-\delta^{18}O$ were shown for four genera at each sampling time. The grey shaded areas in panels **(A–C)** represent nocturnal periods.

explored to assess the long-term benefits of dew at plant (e.g., among species difference) and ecosystem scales.

4.3 Genus variability

Plant water stress can be induced by low soil moisture or high atmospheric water demand ([Liu et al., 2020](#)). In this study, leaf water status of *Poa* was dependent on soil moisture ([Figure 9B](#)),

whilst LWP of *Alchemilla*, *Taraxacum*, and *Trifolium* were mainly controlled by atmospheric humidity conditions ([Figure 9C](#)). Among the four genera, *Poa* was most substantially affected by heat-drought stress as indicated in their lower LWP ([Figure 6](#)), higher $\delta^{18}O_{lw}$ and $\delta^{13}C_{1s}$ ([Figures 7A, 8A, B](#)). This could be induced by the reliance of *Poa* on soil moisture ([Figure 9B](#)), and lower foliar water uptake of *Poa* ([Figure 8D](#)). More severe drought stress of *Poa* induced their lower WUE (higher $\delta^{13}C_{1s}$; [Figure 8F](#)) as compared to *Taraxacum*, and *Trifolium*. Palmately-lobed and hairy leaves of



Alchemilla might prolong the dew water retention on their leaves, and thus induced stronger foliar water uptake (Figure 8D) and slightly increased LWP (Figure 6) compared to the other three genera.

Both *Alchemilla* and *Trifolium* depended on shallower soil water depth (Figure 7B), but they probably benefited from dew water to maintain their plant water status (Figure 6) in response to heat and drought stress. In the case of *Trifolium*, the hairy trichomes on the edges of the leaves probably promoted foliar water uptake (Figure 8D). Many high-elevation plants have hairy structures to help reduce water loss, reflect excess radiation, and protect plants from pathogens (Zeng

et al., 2013; Hamaoka et al., 2017). The control experiment at the same site by Prechsl et al. (2015) found that C_3 -grasses did not shift to deeper soil water under drought treatment, indicating that high-elevation plants could benefit from leaf structures regulating their energy and water balances. On the contrary, with deeper soil water sources, the plant water status of *Poa* strongly declined (Figure 6) in response to heat-drought stress. The maintenance of *Taraxacum* LWP (Figure 6) in response to heat-drought stress might be beneficial from their waxy leaf surfaces (Figure S1) and deeper soil water uptake (Figure 7B). These results indicated that both soil moisture and atmospheric conditions can affect the ecosystem carbon and water exchange

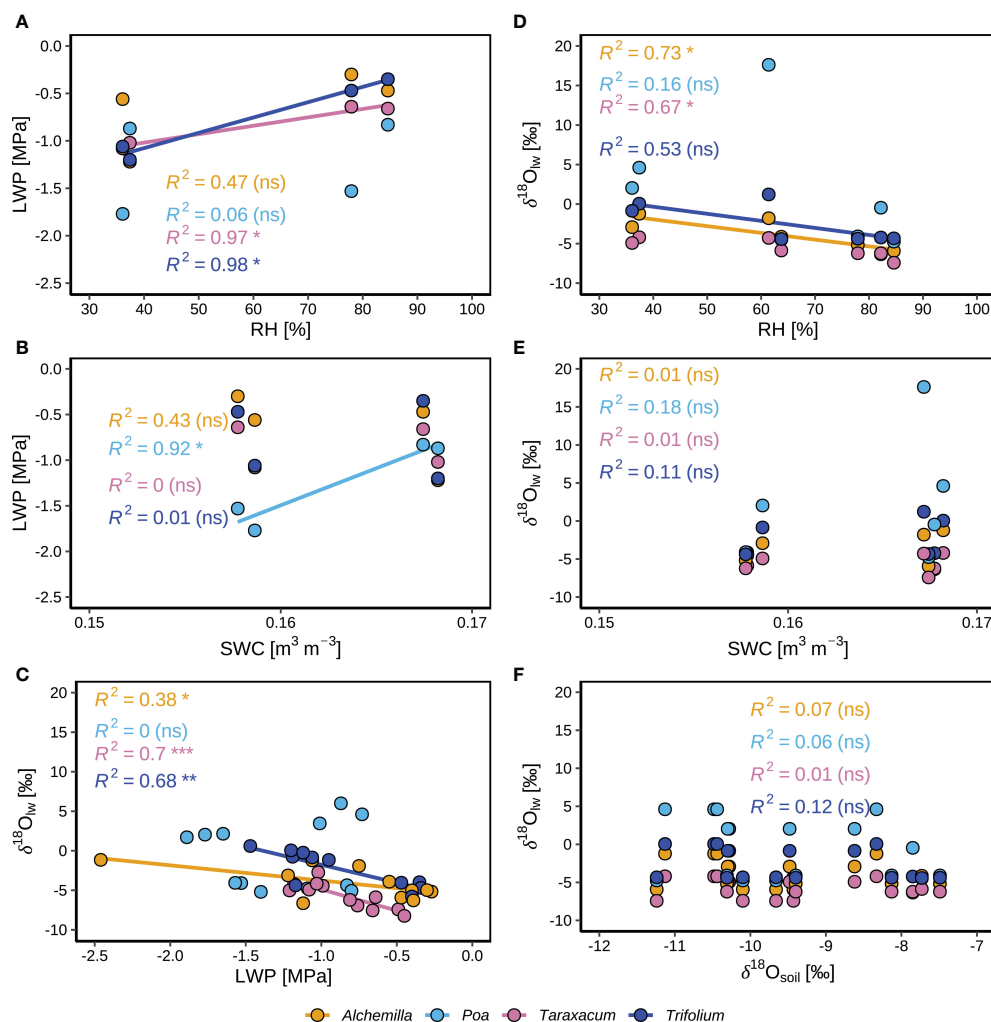
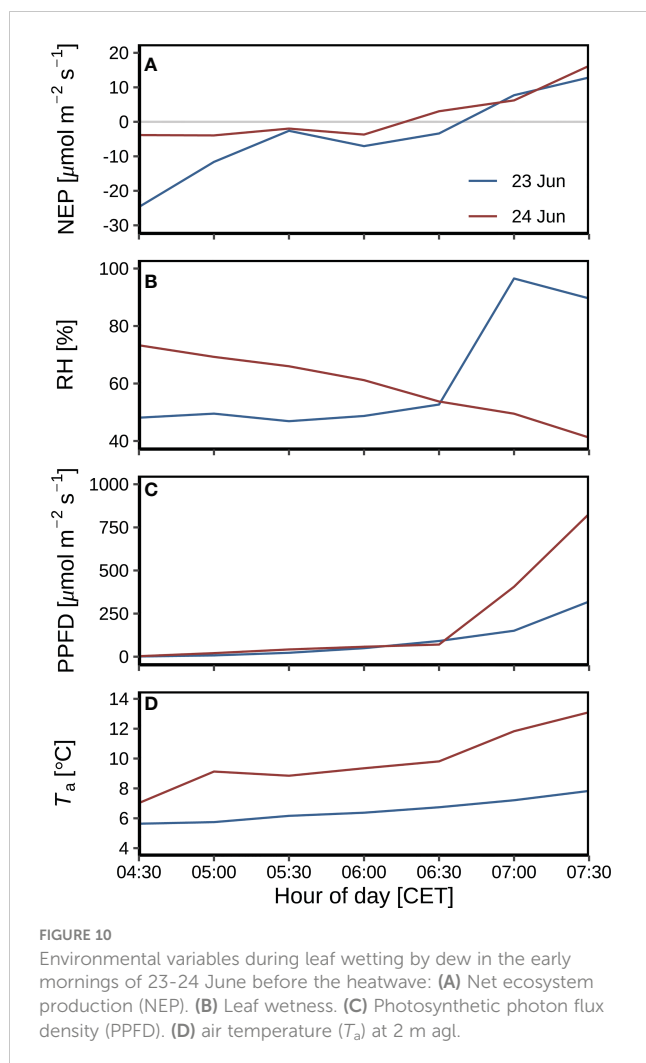


FIGURE 9

Correlations between different environmental and plant variables for four plant genera (*Alchemilla*, *Poa*, *Taraxacum*, and *Trifolium*) during two consecutive intensive observation periods (IOP1 and IOP2) with nocturnal dew formation at the end of the June 2019 heatwave: (A) Median leaf water potential (LWP) and corresponding relative humidity (RH, at 2 m agl). (B) Median LWP and corresponding volumetric soil water content (SWC) at 5 cm depth. (C) Leaf water isotopes ($\delta^{18}\text{O}_{\text{lw}}$) and LWP. (D) Median $\delta^{18}\text{O}_{\text{lw}}$ and corresponding RH. (E) Median $\delta^{18}\text{O}_{\text{lw}}$ and corresponding SWC. (F) Median $\delta^{18}\text{O}_{\text{lw}}$ and median soil water isotopes ($\delta^{18}\text{O}_{\text{soil}}$).

under heat-drought stressed conditions through their varied influence on different plant genera. Due to the similar $\delta^{18}\text{O}$ values for dew and soil water (Figure 7B), we could not split the contributions of dew (foliar water uptake) and nighttime plant tissue refilling (root water uptake; Schulze et al., 2019) on plant water status using the natural-conditioned data, because both root water uptake and foliar water uptake could occur during nighttime, and dew water can also drip off to the soil (Dawson, 1998) and disturb the isotopic signal of root water uptake fluxes. But our chamber-tracer experiment indicated that the contribution of dew on leaf water can vary from 3% to 14% (Figure 8D). We did not isolate the soil from the vegetation when amending tracer on the grassland plots, hence the tracer could have been directly applied on the soil, and the tracer sprayed on leaf surfaces could also have dripped into the soil. But according to the slight

depletion of $\delta^{18}\text{O}_{\text{lw}}$ in our chamber-tracer experiment, the drip-off effect of dew was probably minor compared to direct foliar uptake of dew and atmospheric water vapor. Based on the facts of similar isotopic signal of dew and soil moisture in natural conditions, previous research used excised leaves and isotopically depleted/enriched water to distinguish the two (root and foliar) water sources (Kim and Lee, 2011; Goldsmith et al., 2017). However, these controlled experiments were performed with self-made chambers acting as a heat trap preventing radiative cooling, which is the most important driver of dew formation in natural conditions (Curtis, 1936; Li et al., 2023), and may thus not reflect natural conditions. Future research should therefore apply approaches that allow to estimate the dew influence on plant water under varying soil moisture conditions in the field (Li et al., 2021).



5 Conclusions

The combination of stable isotope analyses in meteoric waters and leaf sugars, meteorological and plant physiological measurements, complemented by eddy-covariance fluxes for H_2O vapor and CO_2 provided novel insights into the effects of combined heat-drought stress on the water and carbon exchange of an alpine grassland.

- (1) Before the heatwave, NEP increased with RH levels, but the dew benefits were cancelled out during the heatwave. NEP decreased with RH levels at the beginning of the heatwave, and showed no significant correlation with leaf wetness at the later stages of the heatwave.
- (2) The isotope signal of amended dew in the chamber tracer experiment was not transferred to leaf sugar, indicating that dew water did not participate in the carbon assimilation. The minor effect of dew on NEP might be derived from low contribution (3-14%) of dew in leaf water, and the partial stomatal closure induced by heat-drought stress.

- (3) NEP reduction was most severe on the hottest two days, with the shift from net ecosystem uptake to net ecosystem emission on the second hottest day just after the peak of the heatwave, indicating that the heat effect was intensified by drought stress.
- (4) The recovery of NEP after the peak of the heatwave indicated the regrowth ability of alpine plants. Plants benefited from the minor effect of heat-drought stress on their water status, which could be recovered *via* the refilling of plant tissues during nighttime.
- (5) The among-genera difference of leaf water status and isotopes in response to heat-drought stress and dew occurrence indicated the varied controls of soil moisture and atmospheric evaporative demand on plant water status, with soil-dependent genera suffering from more severe drought stress compared to the atmospheric-reliant genera.

Our results thus reveal that dew influence on ecosystem water and carbon exchange varied by the levels and stages of environmental stress and plant physiology.

Data availability statement

The datasets presented in this study can be found in the ETH Zurich research collection at <https://doi.org/10.3929/ethz-b-000537314>.

Author contributions

YL, WE, AR, and ML designed the experiment. YL conducted the field and laboratory work. YL and ML performed the purification of plant sugars. YL wrote and revised the manuscript, with contributions and feedback from NB, WE, ML, FA and AR. All authors contributed to the article and approved the submitted version. WE passed away on 23 May 2022 before the final submission of this study.

Funding

This study was funded by the Swiss National Science Foundation (grant no. 175733). We also acknowledge funding from the EU project SUPER-G (Developing SUSTainable PERmanent Grassland systems and policies; project 774124) and open access funding by ETH Zurich. ML was funded by the Swiss National Science Foundation (grant no. 179978).

Acknowledgments

We thank Dr. Lukas Hörtnagl (Grassland Sciences group at ETH Zurich) and Dr. Shiva Ghiasi (Agroscope, the Swiss Center of Excellence for Agricultural Research) for flux data processing. We thank Annika Ackermann and Dr. Roland A. Werner (Grassland Sciences group at ETH Zurich) as well as Manuela Oettli and Dr.

Matthias Saurer (Stable Isotope Research Center at WSL Birmensdorf) for their assistance with isotope analyses. We further thank Oliver Rehmann at WSL for laboratory assistance, Tobia Lezuo at ETH Zurich for field work, as well as the AgroVet-Strickhof staff (Eschikon, Switzerland) and the technician team of the Grassland Sciences group for their field site support.

Conflict of interest

The authors declare that the research was conducted in the absence of any commercial or financial relationships that could be construed as a potential conflict of interest.

References

- Aubinet, M., Vesala, T., and Papale, D. (2012). *Eddy covariance: a practical guide to measurement and data analysis* (Dordrecht: Springer). doi: 10.1007/978-94-007-2351-1
- Bachmann, D., Gockele, A., Ravenek, J. M., Roscher, C., Strecker, T., Weigelt, A., et al. (2015). No evidence of complementary water use along a plant species richness gradient in temperate experimental grasslands. *PLoS One* 10 (1), e0116367. doi: 10.1371/journal.pone.0116367
- Barriopedro, D., Fischer, E. M., Luterbacher, J., Trigo, R. M., and García-Herrera, R. (2011). The hot summer of 2010: redrawing the temperature record map of Europe. *Science* 332 (6026), 220–224. doi: 10.1126/science.1201224
- Beysens, D. (2018). *Dew water* (Denmark: River Publishers).
- Bögelein, R., Lehmann, M. M., and Thomas, F. M. (2019). Differences in carbon isotope leaf-to-phloem fractionation and mixing patterns along a vertical gradient in mature European beech and Douglas fir. *New Phytol.* 222 (4), 1803–1815. doi: 10.1111/nph.15735
- Boucher, J. F., Munson, A. D., and Bernier, P. Y. (1995). Foliar absorption of dew influences shoot water potential and root-growth in pinus-strobus seedlings. *Tree Physiol.* 15 (12), 819–823. doi: 10.1093/treephys/15.12.819
- Brandes, E., Kodama, N., Whittaker, K., Weston, C., Rennenberg, H., Keitel, C., et al. (2006). Short-term variation in the isotopic composition of organic matter allocated from the leaves to the stem of pinus sylvestris: effects of photosynthetic and postphotosynthetic carbon isotope fractionation. *Global Change Biol.* 12 (10), 1922–1939. doi: 10.1111/j.1365-2486.2006.01205.x
- Brewer, C. A., and Smith, W. K. (1994). Influence of simulated dewfall on photosynthesis and yield in soybean isolines (Glycine max [L.] merr. cv williams) with different trichome densities. *Int. J. Plant Sci.* 155 (4), 460–466. doi: 10.1086/297183
- Brilli, F., Hörtnagl, L., Hammerle, A., Haslwanter, A., Hansel, A., Loreto, F., et al. (2011). Leaf and ecosystem response to soil water availability in mountain grasslands. *Agric. For. Meteorology* 151 (12), 1731–1740. doi: 10.1016/j.agrformet.2011.07.007
- Burgess, S. S. O., and Bleby, T. M. (2006). Redistribution of soil water by lateral roots mediated by stem tissues. *J. Exp. Bot.* 57 (12), 3283–3291. doi: 10.1093/jxb/erl085
- Cernusak, L. A., Pate, J. S., and Farquhar, G. D. (2002). Diurnal variation in the stable isotope composition of water and dry matter in fruiting lupinus angustifolius under field conditions. *Plant Cell Environ.* 25 (7), 893–907. doi: 10.1046/j.1365-3040.2002.00875.x
- Ciais, P., Reichstein, M., Viovy, N., Granier, A., Ogee, J., Allard, V., et al. (2005). Europe-Wide reduction in primary productivity caused by the heat and drought in 2003. *Nature* 437 (7058), 529–533. doi: 10.1038/nature03972
- Clus, O., Ortega, P., Muselli, M., Milimouk, I., and Beysens, D. (2008). Study of dew water collection in humid tropical islands. *J. Hydrol* 361 (1-2), 159–171. doi: 10.1016/j.jhydrol.2008.07.038
- Coplen, T. B. (2011). Guidelines and recommended terms for expression of stable-isotope-ratio and gas-ratio measurement results. *Rapid Commun. Mass Spectrometry* 25 (17), 2538–2560. doi: 10.1002/rcm.5129
- Cremonese, E., Filippa, G., Galvagno, M., Siniscalco, C., Oddi, L., di Cella, U. M., et al. (2017). Heat wave hinders green wave: the impact of climate extreme on the phenology of a mountain grassland. *Agric. For. Meteorology* 247, 320–330. doi: 10.1016/j.agrformet.2017.08.016
- Curtis, O. F. (1936). Leaf temperatures and the cooling of leaves by radiation. *Plant Physiol.* 11 (2), 343–364. doi: 10.1104/pp.11.2.343
- Dawson, T. E. (1998). Fog in the California redwood forest: ecosystem inputs and use by plants. *Oecologia* 117 (4), 476–485. doi: 10.1007/s004420050683
- Dawson, T. E., and Goldsmith, G. R. (2018). The value of wet leaves. *New Phytol.* 219 (4), 1156–1169. doi: 10.1111/nph.15307
- De Boeck, H. J., Bassin, S., Verlinden, M., Zeiter, M., and Hiltbrunner, E. (2016). Simulated heat waves affected alpine grassland only in combination with drought. *New Phytol.* 209 (2), 531–541. doi: 10.1111/nph.13601
- Dongmann, G., Nurnberg, H. W., Forstel, H., and Wagener, K. (1974). On the enrichment of H₂¹⁸O in the leaves of transpiring plants. *Radiat. Environ. Biophysics* 11 (1), 41–52. doi: 10.1007/BF01323099
- Eugster, W., and Siegrist, F. (2000). The influence of nocturnal CO₂ advection on CO₂ flux measurements. *Basic Appl. Ecol.* 1 (2), 177–188. doi: 10.1078/1439-1791-00028
- Farquhar, G. D., and Lloyd, J. (1993). “Carbon and oxygen isotope effects in the exchange of carbon dioxide between terrestrial plants and the atmosphere,” in *Stable isotopes and plant carbon-water relations*. Eds. J. R. Ehleringer, A. E. Hall and G. D. Farquhar (San Diego: Academic Press), 47–70. doi: 10.1016/B978-0-08-091801-3.50011-8
- Gehre, M., Geilmann, H., Richter, J., Werner, R. A., and Brand, W. A. (2004). Continuous flow ²H/¹H and ¹⁸O/¹⁶O analysis of water samples with dual inlet precision. *Rapid Commun. mass spectrometry* 18 (22), 2650–2660. doi: 10.1002/rcm.1672
- Gerlein-Safdi, C., Gauthier, P. P. G., and Caylor, K. K. (2018). Dew-induced transpiration suppression impacts the water and isotope balances of colocasia leaves. *Oecologia* 187 (4), 1041–1051. doi: 10.1007/s00442-018-4199-y
- Gessler, A., Brandes, E., Keitel, C., Boda, S., Kayler, Z. E., Granier, A., et al. (2013). The oxygen isotope enrichment of leaf-exported assimilates—does it always reflect lamina leaf water enrichment? *New Phytol.* 200 (1), 144–157. doi: 10.1111/nph.12359
- Gharun, M., Hortnagl, L., Paul-Limoges, E., Ghiasi, S., Feigenwinter, I., Burri, S., et al. (2020). Physiological response of Swiss ecosystems to 2018 drought across plant types and elevation. *Philos. T R Soc. B* 375 (1810), 20190521. doi: 10.1098/rstb.2019.0521
- Goldsmith, G. R., Lehmann, M. M., Cernusak, L. A., Arend, M., and Siegwolf, R. T. W. (2017). Inferring foliar water uptake using stable isotopes of water. *Oecologia* 184 (4), 763–766. doi: 10.1007/s00442-017-3917-1
- Hamaoka, N., Yasui, H., Yamagata, Y., Inoue, Y., Furuya, N., Araki, T., et al. (2017). A hairy-leaf gene, BLANKET LEAF, of wild oryza nivara increases photosynthetic water use efficiency in rice. *Rice* 10 (1), 20. doi: 10.1186/s12284-017-0158-1
- Hammerle, A., Haslwanter, A., Schmitt, M., Bahn, M., Tappeiner, U., Cernusca, A., et al. (2007). Eddy covariance measurements of carbon dioxide, latent and sensible energy fluxes above a meadow on a mountain slope. *Bound-Lay Meteorol* 122 (2), 397–416. doi: 10.1007/s10546-006-9109-x
- Hanba, Y. T., Moriya, A., and Kimura, K. (2004). Effect of leaf surface wetness and wettability on photosynthesis in bean and pea. *Plant Cell Environ.* 27 (4), 413–421. doi: 10.1046/j.1365-3040.2004.01154.x
- Hiller, R., Zeeman, M. J., and Eugster, W. (2008). Eddy-covariance flux measurements in the complex terrain of an alpine valley in Switzerland. *Bound-Lay Meteorol* 127 (3), 449–467. doi: 10.1007/s10546-008-9267-0
- Horiguchi, I., Sugaya, H., and Tani, H. (1982). The measurement of longwave radiation properties upon plastic films used in greenhouses. *J. Agric. Meteorology* 38 (1), 9–14. doi: 10.2480/agrmet.38.9
- Horita, J., and Wesolowski, D. J. (1994). Liquid-vapor fractionation of oxygen and hydrogen isotopes of water from the freezing to the critical temperature. *Geochimica Cosmochimica Acta* 58 (16), 3425–3437. doi: 10.1016/0016-7037(94)90096-5

Publisher's note

All claims expressed in this article are solely those of the authors and do not necessarily represent those of their affiliated organizations, or those of the publisher, the editors and the reviewers. Any product that may be evaluated in this article, or claim that may be made by its manufacturer, is not guaranteed or endorsed by the publisher.

Supplementary material

The Supplementary Material for this article can be found online at: <https://www.frontiersin.org/articles/10.3389/fpls.2023.1136037/full#supplementary-material>

- IAEA (2009). Reference sheet for VSMOW2 and SLAP2 international measurement standards. *Int. Atomic Energy Agency (IAEA) Vienna Austria* pp. 8. Available at: https://nucleus.iaea.org/sites/ReferenceMaterials/Shared%20Documents/ReferenceMaterials/StableIsotopes/VSMOW2/VSMOW2_SLAP2.pdf.
- Jacobs, A. F. G., Heusinkveld, B. G., Kruit, R. J. W., and Berkowicz, S. M. (2006). Contribution of dew to the water budget of a grassland area in the Netherlands. *Water Resour. Res.* 42 (3), W03415. doi: 10.1029/2005WR004055
- Keller, P. (2006). *Vegetationskundliche Untersuchungen und Ertrag der Grünlandflächen im Gebiet der ETH-Forschungsstation Alp Weissenstein GR* (Zurich, Switzerland: University of Zurich), 119 pp.
- Kim, K., and Lee, X. (2011). Transition of stable isotope ratios of leaf water under simulated dew formation. *Plant Cell Environ.* 34 (10), 1790–1801. doi: 10.1111/j.1365-3040.2011.02375.x
- Lehmann, M. M., Goldsmith, G. R., Mirande-Ney, C., Weigt, R. B., Schonbeck, L., Kahmen, A., et al. (2020). The ^{18}O -signal transfer from water vapour to leaf water and assimilates varies among plant species and growth forms. *Plant Cell Environ.* 43 (2), 510–523. doi: 10.1111/pce.13682
- Lehmann, M. M., Goldsmith, G. R., Schmid, L., Gessler, A., Saurer, M., and Siegwolf, R. T. W. (2018). The effect of ^{18}O -labelled water vapour on the oxygen isotope ratio of water and assimilates in plants at high humidity. *New Phytol.* 217 (1), 105–116. doi: 10.1111/nph.14788
- Li, Y., Aemisegger, F., Riedl, A., Buchmann, N., and Eugster, W. (2021). The role of dew and radiation fog inputs in the local water cycling of a temperate grassland during dry spells in central Europe. *Hydrol. Earth Syst. Sci.* 25 (5), 2617–2648. doi: 10.5194/hess-25-2617-2021
- Li, Y., Riedl, A., Eugster, W., Buchmann, N., Cernusak, L. A., Lehmann, M. M., et al. (2023). The role of radiative cooling and leaf wetting in air–leaf water exchange during dew and radiation fog events in a temperate grassland. *Agric. For. Meteorology* 328, 109256. doi: 10.1016/j.agrformet.2022.109256
- Li, L. F., Zheng, Z. Z., Biederman, J. A., Qian, R. Y., Ran, Q. W., Zhang, B., et al. (2020). Drought and heat wave impacts on grassland carbon cycling across hierarchical levels. *Plant Cell Environ.* doi: 10.1111/pce.13767
- LI-COR (2019). *Eddy covariance processing software (Version 7.0.6)* (Bad Homburg, Germany: LI-COR. LI-COR, Inc). Available at: https://www.licor.com/env/products/eddy_covariance/software.html.
- Limm, E. B., Simonin, K. A., Bothman, A. G., and Dawson, T. E. (2009). Foliar water uptake: a common water acquisition strategy for plants of the redwood forest. *Oecologia* 161 (3), 449–459. doi: 10.1007/s00442-009-1400-3
- Liu, L., Gudmundsson, L., Hauser, M., Qin, D., Li, S., and Seneviratne, S. I. (2020). Soil moisture dominates dryness stress on ecosystem production globally. *Nat. Commun.* 11 (1), 4892. doi: 10.1038/s41467-020-18631-1
- Maier, R., Hörtnagl, L., and Buchmann, N. (2022). Greenhouse gas fluxes (CO_2 , N_2O and CH_4) of pea and maize during two cropping seasons: drivers, budgets, and emission factors for nitrous oxide. *Sci. Total Environ.* 849, 157541. doi: 10.1016/j.scitotenv.2022.157541
- MeteoSwiss. (2019). “Climate bulletin summer 2019.” In: *Federal Office for Meteorology and Climatology MeteoSwiss*. Available at: https://www.meteoswiss.admin.ch/home/search.subpage.html/en/data/publications/2019/9/klimabulletin-sommer-2019.html?pageIndex=1&query=Climate%20bulletin%20summer%202019&tab=search_tab.
- Michna, P., Eugster, W., Hiller, R. V., Zeeman, M. J., and Wanner, H. (2013). Topoclimatological case-study of alpine pastures near the alba pass in the eastern Swiss Alps. *Geogr. Helv.* 68 (4), 249–263. doi: 10.5194/gh-68-249-2013
- Mitchell, D., Kornhuber, K., Huntingford, C., and Uhe, P. (2019). The day the 2003 European heatwave record was broken. *Lancet Planetary Health* 3 (7), e290–e292. doi: 10.1016/S2542-5196(19)30106-8
- Oliveira, B. R. F., Schaller, C., Keizer, J. J., and Foken, T. (2021). Estimating immediate post-fire carbon fluxes using the eddy-covariance technique. *Biogeosciences* 18 (1), 285–302. doi: 10.5194/bg-18-285-2021
- Overpeck, J. T. (2013). Climate science: the challenge of hot drought. *Nature* 503 (7476), 350–351. doi: 10.1038/503350a
- Prechsl, U. E., Burri, S., Gilgen, A. K., Kahmen, A., and Buchmann, N. (2015). No shift to a deeper water uptake depth in response to summer drought of two lowland and sub-alpine C_3 -grasslands in Switzerland. *Oecologia* 177 (1), 97–111. doi: 10.1007/s00442-014-3092-6
- Prechsl, U. E., Gilgen, A. K., Kahmen, A., and Buchmann, N. (2014). Reliability and quality of water isotope data collected with a lowbudget rain collector. *Rapid Commun. Mass Spectrometry* 28 (8), 879–885. doi: 10.1002/rcm.6852
- R Core Team (2021). *R: a language and environment for statistical computing* (Vienna, Austria: R Foundation for Statistical Computing).
- Riedl, A., Li, Y., Eugster, J., Buchmann, N., and Eugster, W. (2022). High-accuracy weighing micro-lysimeter system for long-term measurements of non-rainfall water inputs to grasslands. *Hydrology and Earth System Sciences* 26(1), 91–116. doi: 10.5194/hess-26-91-2022
- Rinne, K. T., Saurer, M., Streit, K., and Siegwolf, R. T. W. (2012). Evaluation of a liquid chromatography method for compound-specific $\delta^{13}\text{C}$ analysis of plant carbohydrates in alkaline media. *Rapid Commun. Mass Spectrometry* 26 (18), 2173–2185. doi: 10.1002/rcm.6334
- Schulze, E., Beck, E., Buchmann, N., Clemens, S., Müller-Hohenstein, M., and Scherer-Lorenzen, M. (2019). *Plant ecology* (Heidelberg, Germany: Springer Berlin, Heidelberg). doi: 10.1007/978-3-662-56233-8
- Siegwolf, R., Lehmann, M., Goldsmith, G., Churakova, O., Mirande-Ney, C., Gruspante, G., et al. (2021). The dual c and O isotope–gas exchange model: a concept review for understanding plant responses to the environment and its application in tree rings. *Authorea Preprints*. doi: 10.22541/au.163844646.68129291/v1
- Simonin, K. A., Santiago, L. S., and Dawson, T. E. (2009). Fog interception by sequoia sempervirens (D. don) crowns decouples physiology from soil water deficit. *Plant Cell Environ.* 32 (7), 882–892. doi: 10.1111/j.1365-3040.2009.01967.x
- Steel, R. G. (1997). *Principles and procedures of statistics a biometrical approach* (Auckland: McGraw-Hill Kogakusha, Ltd.), 633 pp.
- Stull, R. B. (1988). “Stable boundary layer,” in *An introduction to boundary layer meteorology*. Ed. R. B. Stull (Dordrecht: Springer, Dordrecht), 499–543. doi: 10.1007/978-94-009-3027-8_12
- Teuling, A. J., Seneviratne, S. I., Stöckli, R., Reichstein, M., Moors, E., Ciais, P., et al. (2010). Contrasting response of European forest and grassland energy exchange to heatwaves. *Nat. Geosci.* 3 (10), 722–727. doi: 10.1038/ngeo950
- Uclés, O., Villagarcía, L., Cantón, Y., and Domingo, F. (2013). Microlysimeter station for long term non-rainfall water input and evaporation studies. *Agri. For. Meteorology* 182, 13–20. doi: 10.1016/j.agrformet.2013.07.017
- Wang, A., Siegwolf, R. T. W., Joseph, J., Thomas, F. M., Werner, W., Gessler, A., et al. (2021). Effects of soil moisture, needle age and leaf morphology on carbon and oxygen uptake, incorporation and allocation: a dual labeling approach with $^{13}\text{CO}_2$ and H_2^{18}O in foliage of a coniferous forest. *Tree Physiol.* 41 (1), 50–62. doi: 10.1093/treephys/tpaa114
- Werner, R. A., and Brand, W. A. (2001). Referencing strategies and techniques in stable isotope ratio analysis. *Rapid Commun. Mass Spectrometry* 15 (7), 501–519. doi: 10.1002/rcm.258
- WMO (2019). *European Heatwave sets new temperature records* (Geneva, Switzerland: World Meteorological Organization).
- Wolf, S., Eugster, W., Ammann, C., Häni, M., Zielis, S., Hiller, R., et al. (2013). Contrasting response of grassland versus forest carbon and water fluxes to spring drought in Switzerland. *Environ. Res. Lett.* 8 (3), 35007. doi: 10.1088/1748-9326/8/3/035007
- Yakir, D., and Deniro, M. J. (1990). Oxygen and hydrogen isotope fractionation during cellulose metabolism in *Lemna-Gibba* l. *Plant Physiol.* 93 (1), 325–332. doi: 10.1104/pp.93.1.325
- Zeeman, M. J., Hiller, R., Gilgen, A. K., Michna, P., Plüss, P., Buchmann, N., et al. (2010). Management and climate impacts on net CO_2 fluxes and carbon budgets of three grasslands along an elevational gradient in Switzerland. *Agric. For. Meteorology* 150 (4), 519–530. doi: 10.1016/j.agrformet.2010.01.011
- Zeng, Y., Zhu, Y., Lian, L., Xie, H., Zhang, J., and Xie, H. (2013). Genetic analysis and fine mapping of the pubescence gene GL6 in rice (*Oryza sativa* L.). *Chin. Sci. Bull.* 58 (24), 2992–2999. doi: 10.1007/s11434-013-5737-y
- Zscheischler, J., and Fischer, E. M. (2020). The record-breaking compound hot and dry 2018 growing season in Germany. *Weather Clim Extreme* 29, 100270. doi: 10.1016/j.wace.2020.100270
- Zscheischler, J., Martius, O., Westra, S., Bevacqua, E., Raymond, C., Horton, R. M., et al. (2020). A typology of compound weather and climate events. *Nat. Rev. Earth Env.* 1 (7), 333–347. doi: 10.1038/s43017-020-0060-z
- Zschenderlein, P., Fragkoulidis, G., Fink, A. H., and Wirth, V. (2018). Large-Scale rossby wave and synoptic-scale dynamic analyses of the unusually late 2016 heatwave over Europe. *Weather* 73 (9), 275–283. doi: 10.1002/wea.3278